

AD-A071 975

PRATT AND WHITNEY AIRCRAFT GROUP WEST PALM BEACH FL 6--ETC F/G 21/5  
BLADED DISK DYNAMIC RESPONSE.(U)  
FEB 79 J L BEARDEN

F33615-77-C-2093

UNCLASSIFIED

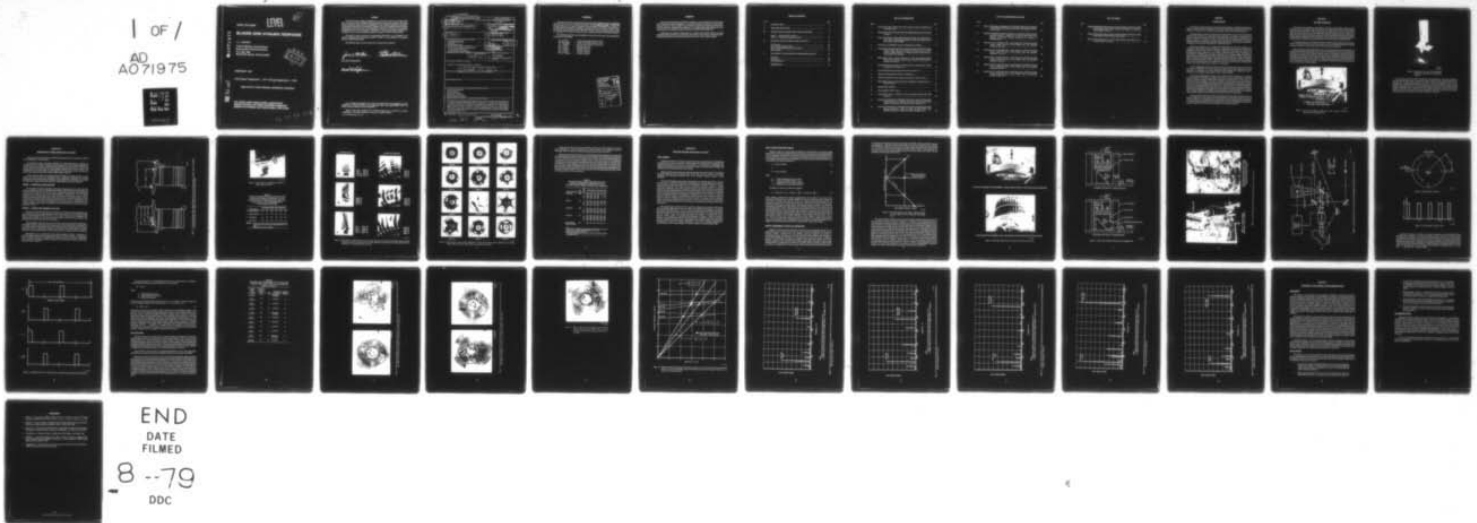
PWA-FR-10576

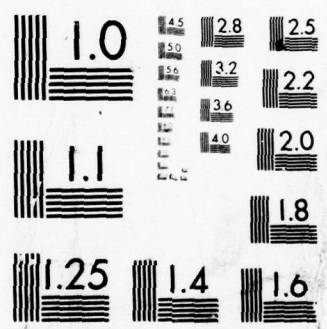
AFAPL-TR-79-2002

NL

1 OF 1

AD  
A071975





DA071975

AFAPL-TR-79-2002

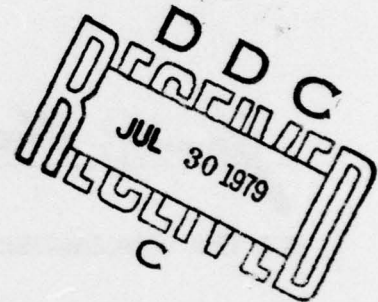
LEVEL

22

## BLADED DISK DYNAMIC RESPONSE

J. L. Bearden

Pratt & Whitney Aircraft Group  
Government Products Division  
P.O. Box 2691  
West Palm Beach, Florida 33402



FEBRUARY 1979

Final Report September 1, 1977 Through September 1, 1978

Approved for Public Release; Distribution Unlimited

AIR FORCE AERO PROPULSION LABORATORY  
UNITED STATES AIR FORCE SYSTEMS COMMAND  
WRIGHT-PATTERSON AIR FORCE BASE, OHIO 45433

DDC FILE COPY

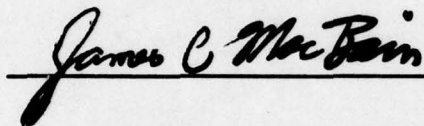
79 07 30 013

## NOTICE

When Government drawings, specifications, or other data are used for any purpose other than in connection with a definitely related Government procurement operation, the United States Government thereby incurs no responsibility nor any obligation whatsoever; and the fact that the government may have formulated, furnished, or in any way supplied the said drawings, specifications, or other data, is not to be regarded by implication or otherwise as in any manner licensing the holder or any other person or corporation, or conveying any rights or permission to manufacture, use, or sell any patented invention that may in any way be related thereto.

This report has been reviewed by the Information Office (OI) and is releasable to the National Technical Information Service (NTIS). At NTIS, it will be available to the general public, including foreign nations.

This technical report has been reviewed and is approved for publication.



FOR THE COMMANDER



If your address has changed, if you wish to be removed from our mailing list, or if the addressee is no longer employed by your organization please notify AFAPL/TBPW-PAFB, OH 45433 to help us maintain a current mailing list.

Copies of this report should not be returned unless return is required by security considerations, contractual obligations, or notice on a specific document.



UNCLASSIFIED

SECURITY CLASSIFICATION OF THIS PAGE (When Data Entered):

19 REPORT DOCUMENTATION PAGE		READ INSTRUCTIONS BEFORE COMPLETING FORM	
1. REPORT NUMBER 18 AFAPL TR-79-2492	2. GOVT ACCESSION NO.	3. RECIPIENT'S CATALOG NUMBER rept.	
4. TITLE (and Subtitle) 6 BLADED DISK DYNAMIC RESPONSE.	5. TYPE OF REPORT & PERIOD COVERED 9 FINAL 1 September 1977 - 1 September 1978	6. PERFORMING ORG. REPORT NUMBER FR-10576	
7. AUTHOR(s) 10 J. L. Bearden	8. CONTRACT OR GRANT NUMBER(s) 15 F33615-77-C-2093	9. PROGRAM ELEMENT, PROJECT, TASK AREA & WORK UNIT NUMBER 16 2307 S2 04	17 S2
10. PERFORMING ORGANIZATION NAME AND ADDRESS Pratt & Whitney Aircraft Group Government Products Division P.O. Box 2691 West Palm Beach, FL 33402	11. CONTROLLING OFFICE NAME AND ADDRESS Air Force Aero Propulsion Laboratory/TBP Air Force Systems Command Wright-Patterson AFB, OH 45433	12. REPORT DATE 11 February 1979	13. NUMBER OF PAGES 38
14. MONITORING AGENCY NAME & ADDRESS (if different from Controlling Office) 12 41 p.	15. SECURITY CLASS. (of this report) UNCLASSIFIED	15a. DECLASSIFICATION/DOWNGRADING SCHEDULE	
16. DISTRIBUTION STATEMENT (of this Report) Approved for public release, distribution unlimited.			
17. DISTRIBUTION STATEMENT (of the abstract entered in Block 20, if different from Report) 14 PWA - FR-10576 61102 F			
18. SUPPLEMENTARY NOTES			
19. KEY WORDS (Continue on reverse side if necessary and identify by block number) Pulsed Laser Holography Optical Derotator Bladed Disk Assembly Electromagnetic Excitation Dynamic Structural Analysis			
20. ABSTRACT (Continue on reverse side if necessary and identify by block number) → The feasibility of applying an optical derotator system to conduct dynamic structural analysis of a rotating/vibrating fully bladed gas turbine rotor assembly in a controlled spin pit facility was investigated. Interferometric holograms using pulsed laser holography were constructed for various assembly modes of vibration at assembly rotational velocities up to 835.6 rad/sec (8000 rpm). Results of this investigation are encouraging although a large bias fringe density resulting from a plexiglass panel in the optical train made definitive analysis of the resultant mode shapes difficult. ←			

DD FORM 1 JAN 73 1473 EDITION OF 1 NOV 65 IS OBSOLETE  
S N 0102-LF-014-6601

UNCLASSIFIED

SECURITY CLASSIFICATION OF THIS PAGE (When Data Entered)

392 887

JUN 79

07 30

213

## FOREWORD

This report details the work performed during the period 1 September 1977 to 1 September 1978 under Air Force Aero Propulsion Laboratory Contract F33615-77-C-2093, "Bladed Disk Dynamic Response," Dr. James C. MacBain, Project Manager. This program was conducted in the Materials and Mechanics Technology Laboratories of Pratt & Whitney Aircraft Group, Government Products Division, West Palm Beach, Florida under the technical direction of Mr. J. L. Bearden, Group Leader, Vibration Analysis, as program manager and principal investigator.

The following personnel are acknowledged for their effort and support which significantly contributed to this program:

Dr. K. Stetson	—	United Technologies Research Center
Mr. Ron Gagosz	—	United Technologies Research Center
Dr. J. MacBain	—	Air Force Aero Propulsion Laboratory
Mr. J. Weber	—	Rotating Structures
Mr. J. Schratt	—	Rotating Structures
Mr. J. Clarady	—	Vibration Analysis
Mr. J. Kramer	—	Vibration Analysis
Mr. W. Thomson	—	Vibration Analysis

Accession For	
NTIS GRI&I	
DDC TAB	
Unannounced	
Justification	
By	
Distribution/	
Availability Codes	
Dist	Avail and/or special

## SUMMARY

This program investigates the feasibility of applying an optical image derotator system and pulsed laser interferometric holography to characterize the dynamic behavior of a gas turbine rotor assembly in a spin pit facility under controlled conditions of steady-state rotation and vibration excitation. Interferometric holograms of a rotating/vibrating fully bladed rotor were constructed at rotor assembly rotational velocities up to 835.6 rad/sec (8000 rpm).

Additionally, the program characterizes and compares the dynamic behavior of single blades mounted individually in a broached test fixture and in a fully bladed rotor assembly under nonrotating conditions and compares this behavior with that of the rotating assembly.

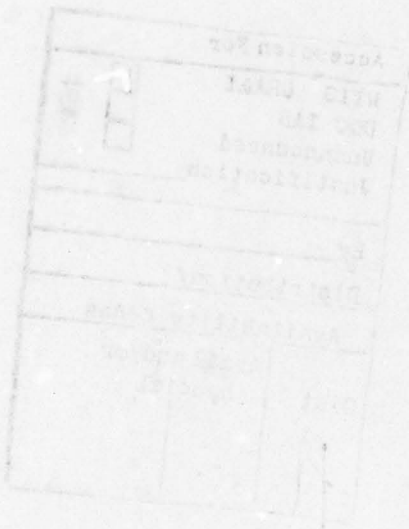




## TABLE OF CONTENTS

<i>Section</i>	<i>Page</i>
I INTRODUCTION.....	1
II THE TEST STRUCTURE.....	2
III NONROTATING DYNAMIC STRUCTURAL ANALYSIS.....	4
Phase I — Individual Blade Analysis.....	4
Phase II — Bladed Disk Assembly Analysis.....	4
IV ROTATING DYNAMIC STRUCTURAL ANALYSIS.....	10
Test Concept.....	10
Disk Dynamic Response Theory.....	11
Spin Pit Experimental Setup and Procedure.....	11
Data Analysis.....	19
V DISCUSSION, CONCLUSIONS AND RECOMMENDATIONS.....	30
Discussion.....	30
Conclusions.....	30
Recommendations.....	31
REFERENCES.....	32

## LIST OF ILLUSTRATIONS

<i>Figure</i>		<i>Page</i>
1	Typical F100 High Turbine Rotor Test Structure Used for Rotating and Nonrotating Tests.....	2
2	Broached Test Fixture With Individual F100 Blade Mounted for Nonrotating Analysis.....	3
3	F100 Second-Stage Turbine Blade Showing Location and Orientation of Strain Gages to Establish Strain/Stress Profile Across Blade Convex and Concave Airfoil at RMT.....	5
4	Test Setup for Holographic Analysis of Bladed Disk Assembly.....	6
5	Photographs of Reconstructed Time Average Holograms of F100 Second-Stage Turbine Blades Showing Comparison of Frequencies and Mode Shapes for Blades Mounted in a Broached Fixture vs Mounted in a Fully Bladed Disk Assembly.....	7
6	Reconstructed Time Average Holograms of F100 Second-Stage Turbine Bladed Disk Assembly Showing Major Response Mode Shapes at Indicated Frequencies.....	8
7	Excitation Frequency for Disk $n^{\text{th}}$ Diameter Mode vs Disk Angular Velocity Neglecting Centrifugal Force.....	12
8	F100 Fully Bladed Rotor Assembly as Mounted in Spin Pit.....	13
9	Present and Proposed PWA Spin Pit Configurations.....	14
10	Optical Component and Code Wheel Arrangement for Spin Pit Tests.....	15
11	Experimental Setup for Image Derotated Holographic Interferometry in a Spin Pit Facility.....	16
12	Rotating Disk Assembly.....	17
13	Force Applied to Disk vs Time.....	17
14	Applied Disk Force vs Position of Force Application During One Disk Revolution.....	18
15	Reconstructed Holograms of F100 High Turbine Rotor Assembly Taken With Assembly Rotating at 7650 rpm (Left) and 7700 rpm (Right) With Response Frequencies of 765 Hz and 770 Hz, Respectively.....	21
16	Reconstructed Holograms of F100 High Turbine Rotor Assembly Taken With Assembly Rotating at 7200 rpm (Left) and 5930 (Right) With Response Frequencies of 960 Hz and 990 Hz, Respectively.....	22



# LIST OF ILLUSTRATIONS (Continued)

<i>Figure</i>		<i>Page</i>
17	Photo of Reconstructed Holograms of F100 High Turbine Rotor Assembly Taken With Assembly Rotating at 6810 rpm With Response Frequency of 1137 Hz.....	23
18	Relation of Resonant Excitation Frequency as a Function of Test Structure Rotational Speed for Modes 2D, 4D, 6D and Blade Alone First Bending and Resonant Response Frequency as a Function of Increasing Speed.....	24
19	Spectrum Plot of Unfiltered Strain Gage Signal from F100 Second-Stage Turbine Blade Mounted in Fully Bladed Disk Test Assembly Rotating at 7650 rpm.....	25
20	Spectrum Plot of Unfiltered Strain Gage Signal from F100 Second-Stage Turbine Blade Mounted in Fully Bladed Disk Test Assembly Rotating at 7710 rpm.....	26
21	Spectrum Plot of Unfiltered Strain Gage Signal from F100 Second-Stage Turbine Blade Mounted in Fully Bladed Disk Test Assembly Rotating at 7200 rpm.....	27
22	Spectrum Plot of Unfiltered Strain Gage Signal from F100 Second-Stage Turbine Blade Mounted in Fully Bladed Disk Test Assembly Rotating at 5930 rpm.....	28
23	Spectrum Plot of Unfiltered Strain Gage Signal from F100 Second-Stage Turbine Blade Mounted in Fully Bladed Disk Test Assembly Rotating at 6810 rpm.....	29

## LIST OF TABLES

<i>Table</i>		<i>Page</i>
1	Dynamic Strain Gage Analysis Data for Indicated Modes of Vibration of F100 Second-Stage Turbine Blades Mounted Individually in a Broached Root Attachment Fixture.....	6
2	Dynamic Strain Gage Analysis Data for Indicated Modes of Vibration of F100 Second-Stage Turbine Bladed Disk Assembly.....	9
3	Dynamic Data Developed for an F100 High Turbine Test Structure in a Controlled Spin Pit Facility.....	20

## SECTION I

### INTRODUCTION

The objective of this program was to determine the feasibility of establishing the dynamic behavior of a gas turbine rotor assembly under controlled conditions of steady-state rotation and vibration by the application of pulsed laser holography and an optical derotator system.

The development of advanced technology gas turbine engines, such as the Pratt & Whitney Aircraft F100, demands the development and application of advanced experimental and analytical analysis techniques. Improved experimental structural analysis to characterize the dynamic behavior of rotating structures, which includes the determination of resonant frequencies, resultant mode shapes, mechanical damping and dynamic stress/strain distribution, is essential for the successful development of rotating structures.

Pulsed and continuous wave interferometric holography has been used routinely as a technique for establishing the response frequencies and resultant mode shapes of structures and preliminary work has been done to determine strain/stress distributions and values from interferometric fringe patterns. For gas turbine engines, the most common application of interferometric holography has been the investigation of the dynamic behavior of individual blade airfoils and bladed disk assemblies under nonrotating conditions. These analyses have greatly improved the understanding of blade and disk interaction under dynamic conditions. There is a serious drawback, however, which limits this form of analyses: body forces resulting from component spinning cannot be applied for a bench test. The only way to simulate these forces is by actually spinning the component or the assembly.

Current experimental dynamic structural analysis of rotating structures is usually based upon either instrumented core or full engine tests, which are extremely expensive and time consuming, or laboratory rig testing. Generally both methods have significant inherent limitations on the quantity and/or quality of the test data obtained.

United Technologies Research Center, under Air Force Contract (Reference 1), developed an optical system incorporating a rotating erector prism with associated controls, which has sufficient precision to enable interferometric holograms of rotating objects to be constructed using pulsed laser holography. The Pratt & Whitney Aircraft Group, Government Products Division, concurrently developed an electromagnetic method (Reference 2) of inducing controlled vibration into a spinning bladed disk assembly. By combining these two methods, holographic studies can be undertaken of actual gas turbine rotors using more realistic controlled conditions. Successful demonstration allows extension of coherent optical metrology techniques to actual gas turbine engine problems of centrifugal strain measurement, rotational effects on vibrational mode response, mechanical and material damping effects and mistuning effects.

This report demonstrates the feasibility of integrating these test methods to characterize the dynamic behavior of a fully bladed, rotating gas turbine rotor assembly subjected to induced vibratory loading in a controlled laboratory environment. The data obtained from this integration is compared to data established for both a single blade and for the fully bladed gas turbine rotor assembly subjected to induced vibratory loading in a nonrotating condition.



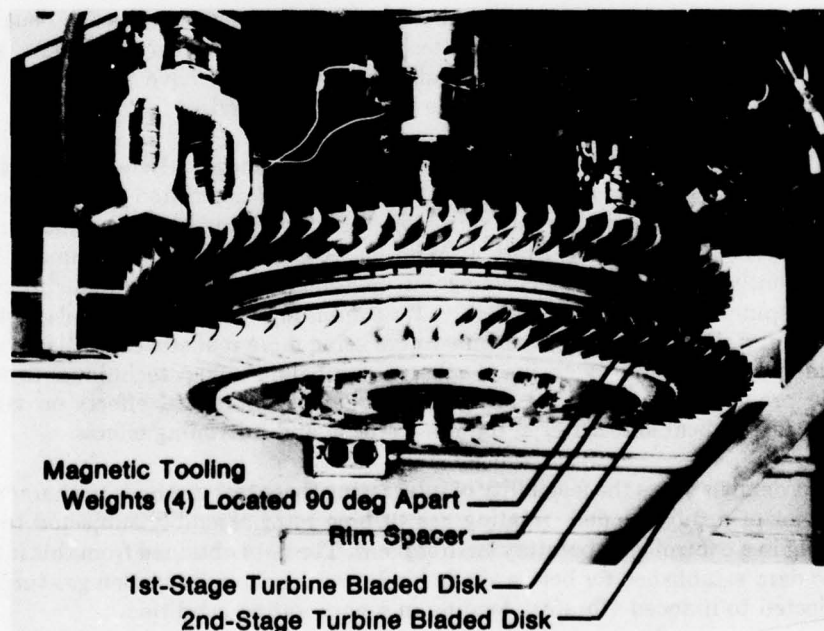
## SECTION II

### THE TEST STRUCTURE

The test structure selected to accomplish the objectives of this program consists of fully bladed F100 first- and second-stage high turbine rotor disks, disk rim spacer and associated hardware as shown in Figure 1. These components were configured as they are in a gas turbine engine with the exception of the second-stage blade platform dampers removed to yield a more responsive structure and four blades removed from the first-stage disk and replaced by magnetic tooling weights to facilitate structural excitation. Of this total structure, the principal elements analyzed were the individual second-stage blades and the fully bladed second-stage disk.

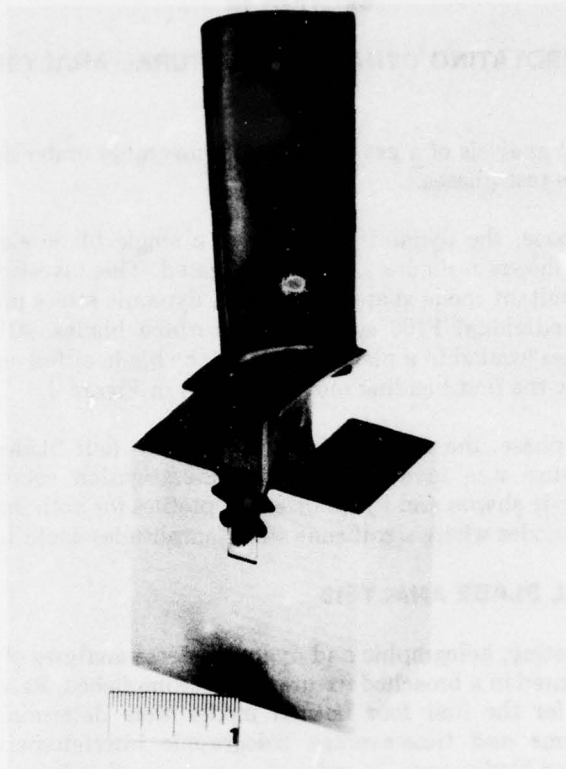
Nonrotating analysis of individual second-stage blades was accomplished by securing each blade in a broached test fixture, as shown in Figure 2, with a simulated centrifugal load applied to the rear of the blade root through a load bar and jackscrew arrangement.

Both nonrotating and rotating analysis of the second-stage fully bladed disk assembly was accomplished using the bladed disk test structure previously described plus the associated spin tooling up to the spin pit drive turbine attachment point. This was done to assure that the test structure was identical in every respect for each test condition. Additionally, all blade root firtree attachments were coated with W. T. Bean Inc. Epoxy Cement type RTC, shimmed (steel shims) at the firtree aft end, driven individually into each disk broached slot and cured at 100°F for one hour. This assembly procedure results in a rigid assembly with good response characteristics for both nonrotating and rotating analyses.



FD 147952

*Figure 1. Typical F100 High Turbine Rotor Test Structure Used for Rotating and Nonrotating Tests*



FE 171318  
FD 147953

*Figure 2. Broached Test Fixture With Individual F100 Blade Mounted for Nonrotating Analysis*

As previously noted, four blades, 90 deg apart circumferentially, were removed from the first-stage disk and replaced by four magnetic tooling weights. For the nonrotating bladed disk analysis, one of these tooling weights provided a convenient attachment point for an electrodynamic shaker which excited the test structure in an axial direction with a variable frequency, sinusoidal input. For the rotating bladed disk analysis, these four magnetic tooling weights, interacting with two stationary dc electromagnets, provided a pulsed vibratory input axially into the test structure with excitation frequency dependent upon the test structures rotational velocity. This excitation method is discussed in Section IV.



## SECTION III

### NONROTATING DYNAMIC STRUCTURAL ANALYSIS

Dynamic structural analysis of a gas turbine rotor assembly under nonrotating conditions was accomplished in two test phases.

In the first test phase, the dynamic behavior of a single blade element, mounted in a broached test fixture as shown in Figure 2, was investigated. This investigation established the response frequencies, resultant mode shapes and airfoil dynamic stress profile for the first four normal modes of four individual F100 second-stage turbine blades. All stress profiles were established by strain gages located in a plane parallel to the blade airfoil chord at the maximum airfoil stress locations for the first bending mode as shown in Figure 3.

In the second test phase, the dynamic behavior of these four blades mounted in a fully bladed disk test structure was investigated. This investigation established the response frequencies, resultant mode shapes and dynamic stress profiles for both individual blade modes and blade-disk coupled modes where significant stress amplitudes could be developed.

#### PHASE I — INDIVIDUAL BLADE ANALYSIS

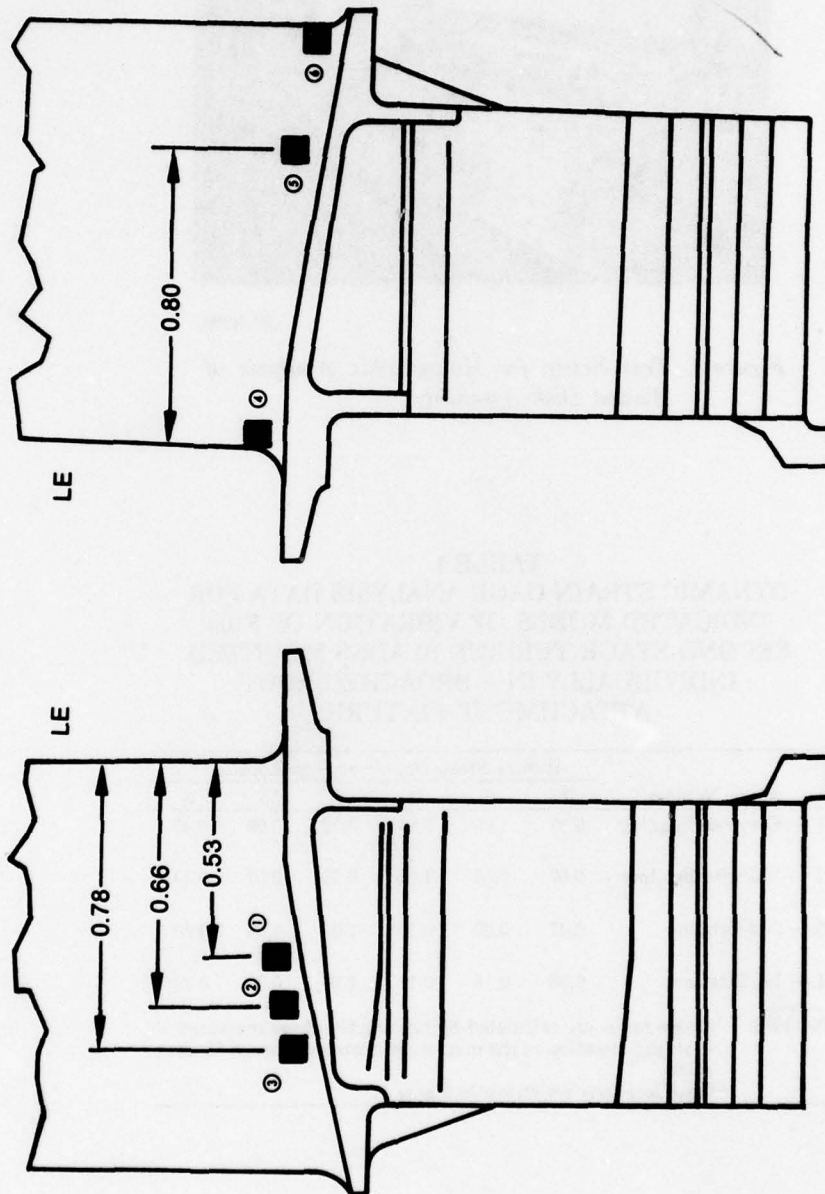
For this phase of testing, holographic and dynamic stress analyses of four individual F100 second-stage blades mounted in a broached fixture were accomplished. Resonant frequencies and resultant mode shapes for the first four normal modes were determined using established continuous wave real-time and time-average holographic interferometry. The four modes identified for each of these blades were, in order of occurrence, first bending easywise, stiffwise bending, second bending and first torsional. Photographs of the reconstructed holograms for each of these modes and their corresponding frequencies are shown in Figure 4. Quantitative stress profiles in terms of stress ratios, as measured at six gage locations, were established for each individual blade in each of the four established modes. The average stress ratio for each mode is presented in Table 1.

#### PHASE II — BLADED DISK ASSEMBLY ANALYSIS

The four instrumented blades analyzed in Phase I were installed in a fully bladed first- and second-stage test structure configured and assembled as described in Section II with these blades located in second-stage disk slot numbers 1, 16, 33, and 53 (90 deg apart). Holographic and dynamic stress analyses of the four instrumented blades mounted in this structure were accomplished using the test setup shown in Figure 4.

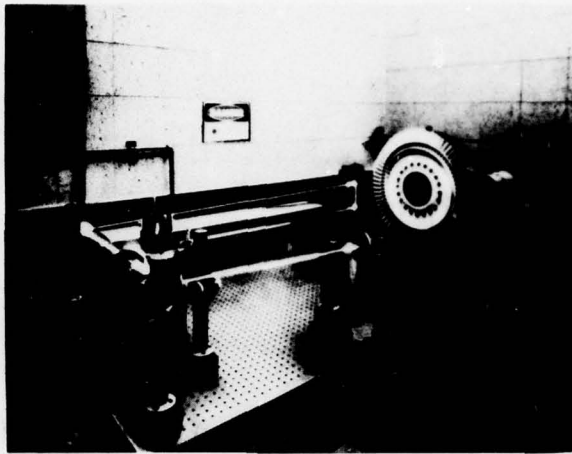
Using established continuous wave real-time and time-average holographic interferometry and standard dynamic stress analysis techniques, analyses of these blades were accomplished to: (1) establish individual blade frequencies, mode shapes and blade stress profiles for the first four blade-alone modes, corresponding to Phase I test results, and (2) establish blade-disk coupled frequencies, resultant mode shapes and blade stress profiles for assembly modes up to 4000 Hz.

Photographs of the reconstructed time-average holograms showing a comparison of individual blade frequencies and resultant mode shapes for blades mounted in a broached test fixture vs blades mounted in the fully bladed test structure are shown in Figure 5. Photographs of reconstructed time-average holograms showing the major blade-disk coupled modes established are shown in Figure 6.



FD 147864

Figure 3. F100 Second-Stage Turbine Blade Showing Location and Orientation of Strain Gages to Establish Strain/Stress Profile Across Blade Convex and Concave Airfoil at RMT



FD 147965

Figure 4. Test Setup for Holographic Analysis of Bladed Disk Assembly

TABLE 1  
DYNAMIC STRAIN GAGE ANALYSIS DATA FOR  
INDICATED MODES OF VIBRATION OF F100  
SECOND-STAGE TURBINE BLADES MOUNTED  
INDIVIDUALLY IN A BROACHED ROOT  
ATTACHMENT FIXTURE

Mode Number	Average Stress Ratio <sup>(1)</sup> at Gage Location <sup>(2)</sup>					
	1	2	3	4	5	6
1 — Easywise Bending	0.97	1.00	0.95	0.72	0.69	0.48
2 — Stiffwise Bending	0.07	0.57	1.00	0.73	0.57	0.14
3 — 2nd-Bending	0.47	0.29	0.15	1.00	0.69	0.80
4 — 1st-Torsional	0.36	0.18	0.19	1.00	0.73	0.79

NOTES: <sup>(1)</sup>Stress ratios are calculated by ratioing the stress measured at each gage location to the maximum stress established for each mode.

<sup>(2)</sup>Gage locations are shown in Figure 1.

**Broached Fixture**



S/N 1 922 Hz  
S/N 2 906 Hz  
TSS 43 923 Hz  
TTE 430 919 Hz



3605 Hz  
3669 Hz  
3618 Hz  
3610 Hz



S/N 1 4076 Hz  
S/N 2 4036 Hz  
TSS 43 3860 Hz  
TTE 430 4057 Hz

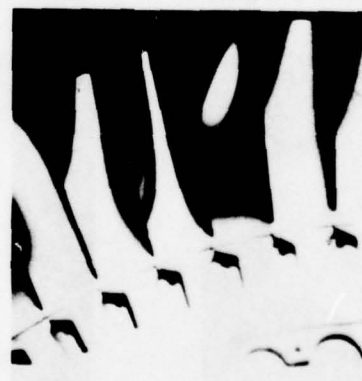
**Bladed Disk Assembly**



915 Hz  
904 Hz  
919 Hz  
920 Hz



3750 Hz  
3323 Hz  
3340 Hz  
3382 Hz

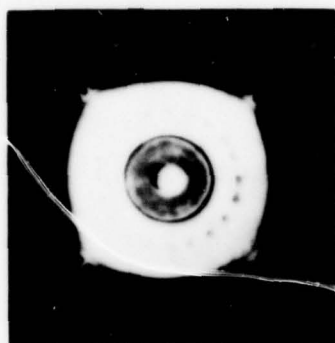


4106 Hz  
3935 Hz  
3874 Hz  
3805 Hz

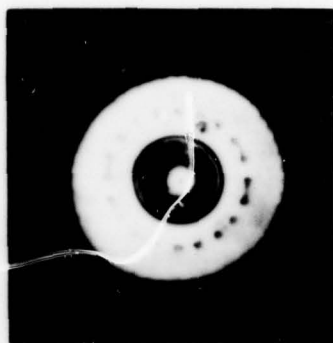
FD 147956

*Figure 5. Photographs of Reconstructed Time Average Holograms of F100 Second-Stage Turbine Blades Showing Comparison of Frequencies and Mode Shapes for Blades Mounted in a Broached Fixture vs Mounted in a Fully Bladed Disk Assembly*

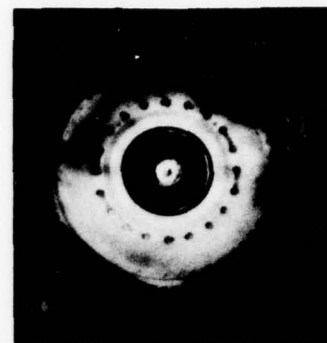




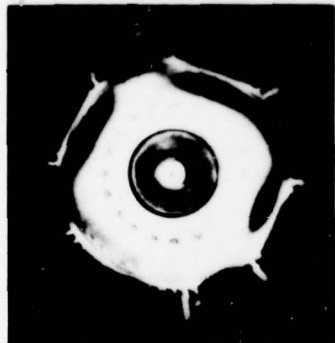
696 Hz



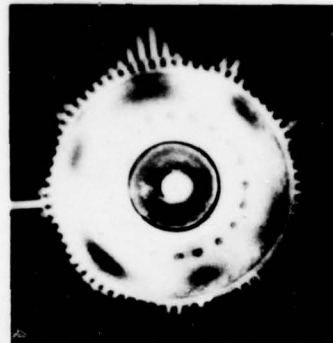
727 Hz



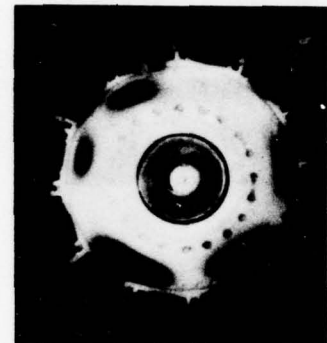
808 Hz



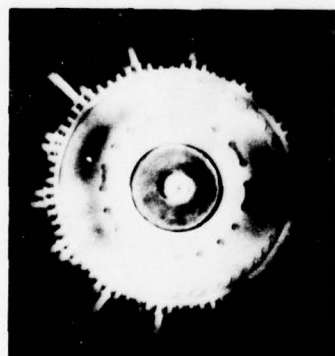
857 Hz



1094 Hz



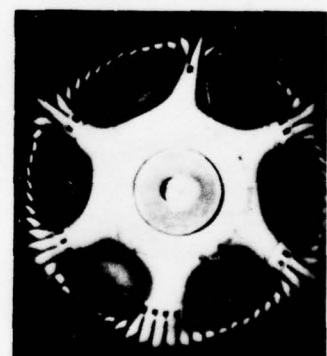
1122 Hz



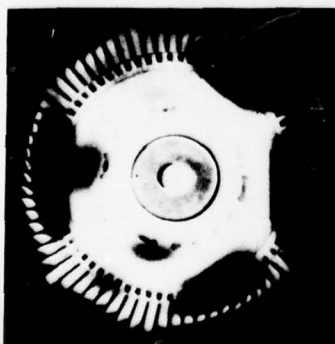
1265 Hz



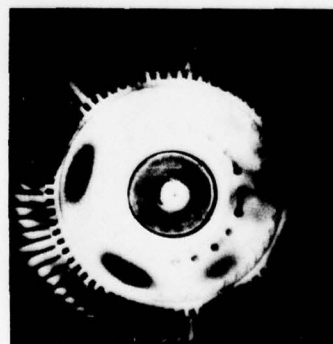
1254 Hz



2543 Hz



2708 Hz



3162 Hz



3815 Hz

FD 147957

Figure 6. Reconstructed Time Average Holograms of F100 Second-Stage Turbine Bladed Disk Assembly Showing Major Response Mode Shapes at Indicated Frequencies



Stress ratios for the four instrumented blades mounted in the fully bladed test structure were established for individual blade modes, where sufficient stress amplitude could be developed, and for the first four blade-disk coupled modes as shown in Table 2.

Analysis of the test data shows that for individual blade response frequencies, not associated with blade-disk coupled modes, blade frequencies and resultant mode shapes are almost identical to those for blades mounted in a broached test fixture. The second mode (stiffwise bending) was not responsive in the test structure, therefore, data for this mode could not be established. Variances in individual blade frequencies between test structure and test fixture mounted blades are attributed to system stiffness and blade root attachment loading differences with the latter being the larger variable. Data analysis also shows that, although the blades are primarily in the flap mode (first easywise bending) for the first four blade-disk coupled modes, their displacement amplitude and stress profile is not the same as those for the individual blade first mode, either in a broached fixture or the test structure.

TABLE 2  
DYNAMIC STRAIN GAGE ANALYSIS DATA FOR  
INDICATED MODES OF VIBRATION OF F100  
SECOND-STAGE TURBINE BLADED DISK ASSEMBLY

Mode of Vibration	Freq. (Hz)	Disk Slot No.	Strain Ratio <sup>(1)</sup> at Gage Location <sup>(2)</sup>					
			1	2	3	4	5	6
2 Nodal Dia.	698	1	0.58	0.81	1.00	0.75	0.15	0.17
		16	0.52	0.81	1.00	0.58	0	0.10
		13	0.59	0.94	1.00	0.29	0	0.12
		53	0.55	0.86	1.00	0.68	0	0
Umbrella	727	1	0.58	0.81	1.00	0.74	0.24	0.26
		16	0.57	0.87	1.00	0.73	0.03	0.07
		33	0.81	1.00	1.00	0.66	0.33	0.39
		53	0.48	0.81	1.00	0.82	0	0
3 Nodal Dia.	808	1	0.72	0.91	1.00	0.74	0.31	0.26
		16	0.72	0.93	1.00	0.73	0.36	0.30
		33	0.86	1.00	0.97	0.66	0.40	0.39
		53	0.78	0.97	1.00	0.82	0.38	0.30
4 Nodal Dia.	857	1	0.62	0.69	1.00	0.75	0.25	0.06
		16	0.77	0.98	1.00	0.72	0.45	0.30
		33	0.91	1.00	0.92	0.63	0.46	0.38
		53	0.83	0.99	1.00	0.82	0.48	0.35
1st Blade Mode <sup>(3)</sup> (Easywise Bending)	914	-	0.96	1.00	0.97	0.79	0.68	0.42

<sup>(1)</sup> Stress ratios are calculated by ratioing the stress measured at each gage location to the maximum stress established for each mode.

<sup>(2)</sup> Gage locations are shown in Figure 1.

<sup>(3)</sup> The frequency and stress ratios for this mode are an average for the four strain gaged blades.

## SECTION IV

### ROTATING DYNAMIC STRUCTURAL ANALYSIS

#### TEST CONCEPT

The dynamic behavior of complex rotating structures, and specifically that of bladed disk structures such as those in modern gas turbine engines, has been the object of analytical and experimental analyses since as early as 1924 (Reference 6). Investigation, understanding and prediction of this behavior has become increasingly imperative with the advent of current and proposed, advanced technology gas turbine engines.

Several analytical and experimental analysis techniques have been applied to investigate the dynamic behavior of high rotational speed, bladed disk structures, however, most of these techniques have significant limitations due to the extremely complex behavior of these structures.

The recent development and successful demonstration of a rotating erector prism, or optical derotator system, combined with pulsed laser, interferometric holography (References 1, 3 and 5), has shown great promise for application in the investigation of dynamic behavior of rotating bladed disk structures. This system optically removes the rotational motion of a rotating structure by passing the image of the structure through a folded Abbe' prism that is rotating at half the structures angular velocity. This causes the structure's image to rotate in the opposite direction at the same angular velocity of the rotating structure thus cancelling the rotational motion. Standard double pulsed holographic interferometry can then be used to record the structure's dynamic response. An electronically controlled, closed-loop, servosystem, using code wheels on both the rotating structure and optical derotator to generate electrical impulses, adjusts the derotator rotational speed to half that of the rotating structure and is phase locked with it. A more rigorous description of the derotator system and analysis technique can be found in Reference 1.

This experimental technique has been applied to relatively small, simple, solid circular disks and pseudo bladed disk and also to a more complex bladed disk assembly in an operating gas turbine engine (References 1, 3 and 5). However, although both applications are of great significance in gaining a better understanding of the dynamic behavior of rotating bladed disks, they are limited in scope. This program investigated the feasibility of applying this optical derotator, double pulsed laser interferometric holography technique to study the dynamic behavior of a fully bladed gas turbine rotor assembly under controlled steady-state rotation and vibration excitation in a spin pit facility. This program was intended to build on the techniques and application of both K. A. Stetson, (References 1 and 3), and J. MacBain, (Reference 5), toward gaining a better understanding of the dynamic behavior of rotating bladed disks.

## DISK DYNAMIC RESPONSE THEORY

Vibratory modes of a circular disk can generally be characterized in two classes; modes symmetrical to the center, having node lines in the form of concentric circles, and unsymmetrical modes with diametrical node lines. Typical disk failure histories indicate that most disk failures can be attributed to vibration of the latter type. Neglecting the effect of centrifugal force, for a disk rotating at angular velocity  $\Omega$  and vibrating in an unsymmetrical mode, disk deflection can be described by the relation (Reference 4):

$$V = V_0 \sin n\theta \cos P_n t \quad (1)$$

or

$$V = V_0 \cos n\theta \sin P_n t \quad (2)$$

where:

- $P_n$  = resonant frequency of the  $n^{\text{th}}$  mode
- $V_0$  = a function of radial distance  $r$  only
- $\theta$  = angular position of a point on the disk
- $n$  = number of  $n^{\text{th}}$  mode nodal diameters

Combining (1) and (2) one obtains the relation:

$$V = V_0 \sin (n\theta \pm P_n t) = V_0 \sin \left( \Omega - \frac{P_n}{n} \right) t + V_0 \sin \left( \Omega + \frac{P_n}{n} \right) t \quad (3)$$

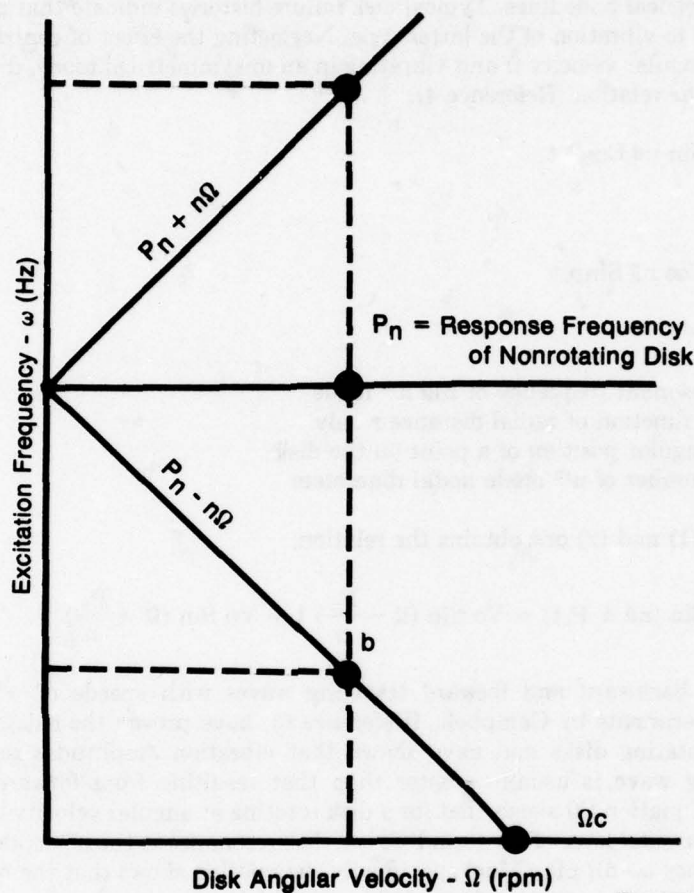
which represent backward and forward traveling waves with speeds of  $-P_n/n$  and  $+P_n/n$  respectively. Experiments by Campbell, (Reference 6), have proven the existence of these two wave trains in rotating disks and have shown that vibration amplitudes resulting from the backward moving wave is usually greater than that resulting from forward moving waves. Examination of Equation (3) shows that for a disk rotating at angular velocity  $\Omega$ , and excited by a nonrotating sinusoidal force of the form  $P \cos \omega t$ , disk resonance in the  $n^{\text{th}}$  mode occurs when the excitation frequency  $\omega = n\Omega \pm P_n$ . More specifically the relation shows that the  $n^{\text{th}}$  disk mode can be excited by at least two excitation frequencies, one which is  $n\Omega$  greater and one which is  $n\Omega$  less than the disks  $n^{\text{th}}$  mode resonant frequency. These resonant conditions are shown graphically as point a and b in Figure 7. Of particular significance is the condition where the speed,  $-P_n/n$ , of the backward moving wave coincides with the forward angular velocity  $\Omega$  of the disk or  $\Omega_c = -P_n/n$  so that the waves are stationary relative to space. At this condition large vibratory amplitudes can be excited by a nonrotating force of zero frequency such as that produced by a dc magnet or nonuniform pressure field across a rotating disk in a gas turbine engine.

## SPIN PIT EXPERIMENTAL SETUP AND PROCEDURE

Analysis of the test structure described in Section II was accomplished during two test periods with the first in December 1977 and the second in July 1978. During the first test period, technical problems, resulting from spin stability, excitation amplitude and method of determining structural resonance were resolved and double pulsed, interferometric holograms of the rotating-vibrating test structure were constructed for at least four modes of vibration. Analysis of the reconstructed holograms revealed a large bias fringe density which made definitive analysis of the structure's excited mode shapes difficult. Analysis of these fringes indicated that the probable cause was either the large front surface mirror located inside the spin pit or the large plexiglass cover over the spin pit vacuum cans which provides viewing access of



the test structure. Based on the opinions of personnel from P&WA, UTRC, and AFAPL and work accomplished by J. MacBain, the large front surface mirror was considered the most probable cause. Therefore, during the second test period the large mirror and mirror mount were replaced by a mirror and mount with much higher structural rigidity. Since the test structure, test procedure and test results were identical during the two test periods, this report will deal primarily with the second period of tests.

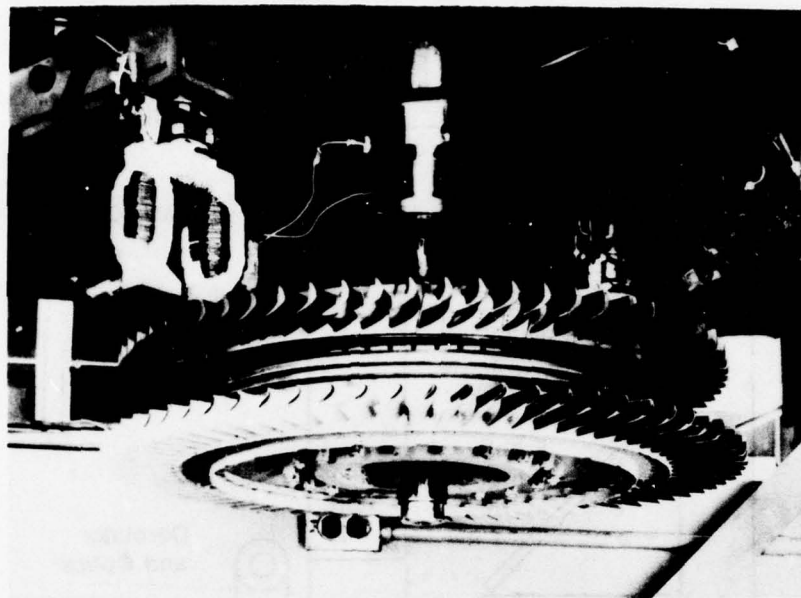


FD 147968

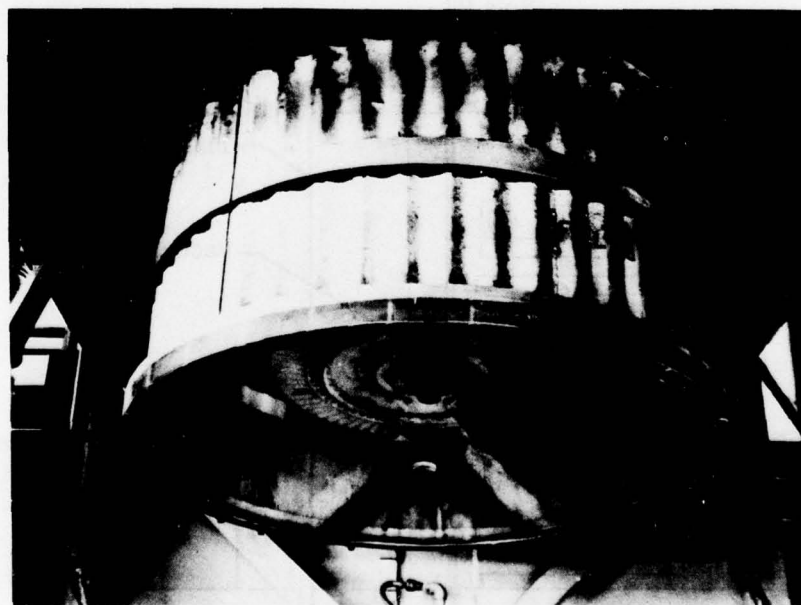
Figure 7. Excitation Frequency for Disk  $n^{\text{th}}$  Diameter Mode vs Disk Angular Velocity Neglecting Centrifugal Force

The optical derotator system and test structure described in Section II was mounted in the spin pit facility as shown in Figures 8 through 10. A diagram of the experimental setup to accomplish image derotated holographic interferometry of the rotating/vibrating test structure is shown in Figure 11. The light from a Q-switched, double pulsed, ruby laser is divided by a 50-50 beam splitter and illuminates the disk via a mirror  $M_1$  which, by virtue of the retroreflective paint on the test structure, is reflected back along the same path where it is reflected by the beam splitter through the derotator to the holographic film. Both the object and reference beam are spread prior to going through the beam splitter. The reference beam passes through the beam splitter to mirror  $M_2$ ,  $M_3$ , and  $M_4$  and on to the holographic film. The film was held and each frame advanced remotely subsequent to each hologram construction by a Jodon film transport. Disk excitation force was provided by the interaction of two stationary dc electromagnets located 180 deg apart and four magnetic tooling weights in the test structure located 90 deg circumferentially apart as shown in Figure 12. Since the magnetic tooling weights are narrow in relation to the total disk circumference, the input force can be approximated for analytical purposes as a series of approximately rectangular pulses as shown in Figure 13.





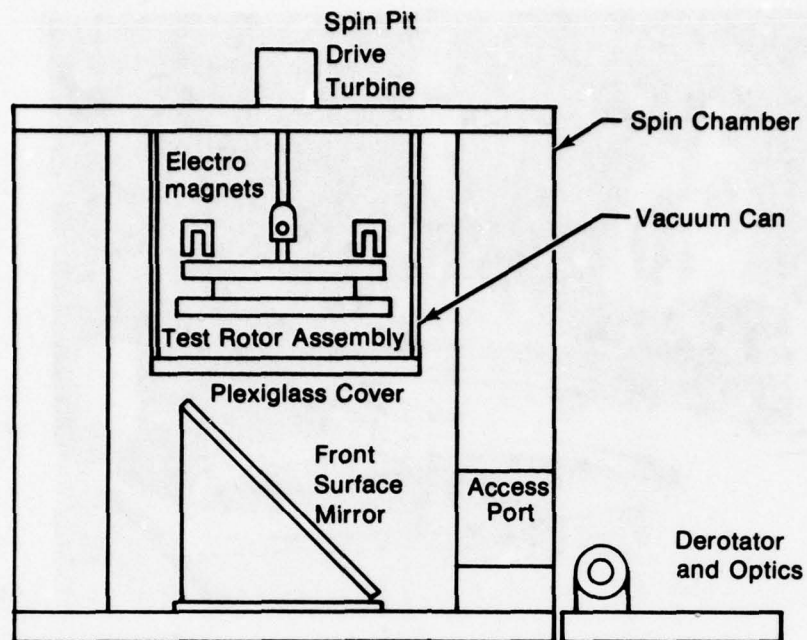
**F100 FULLY BLADED ROTOR ASSEMBLY AS MOUNTED IN SPIN PIT WITH VACUUM CAN REMOVED**



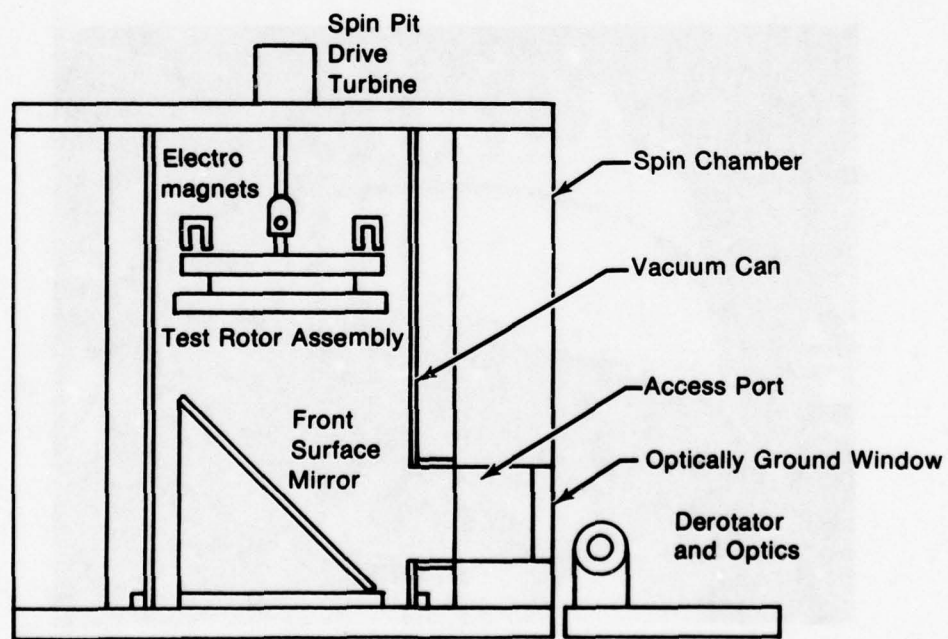
**F100 BLADED DISK ASSEMBLY WITH VACUUM CAN AND PLEXIGLASS COVER IN PLACE**

FD 147959

*Figure 8. F100 Fully Bladed Rotor Assembly as Mounted in Spin Pit*



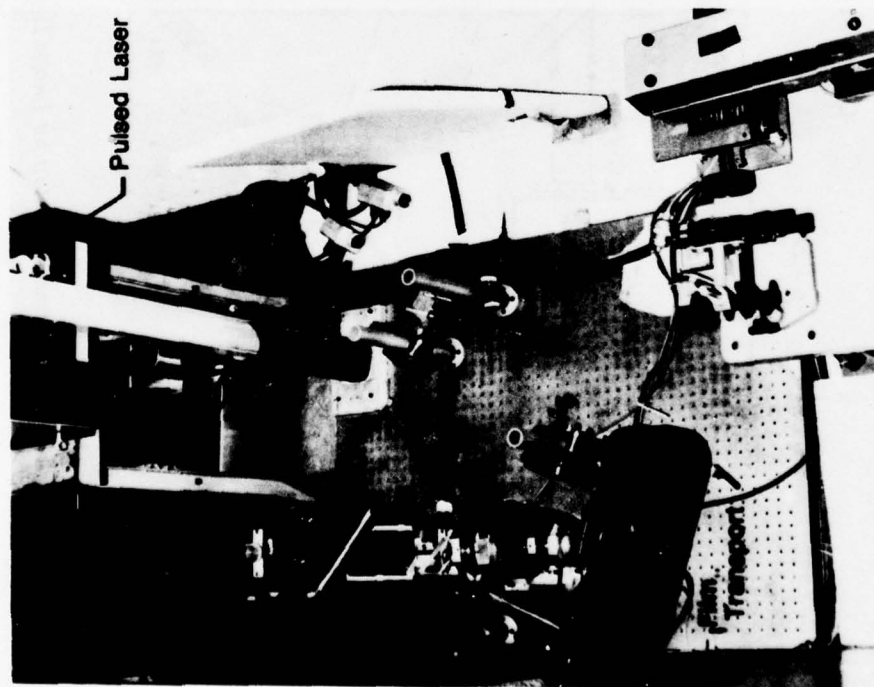
PRESENT PWA SPIN PIT CONFIGURATION



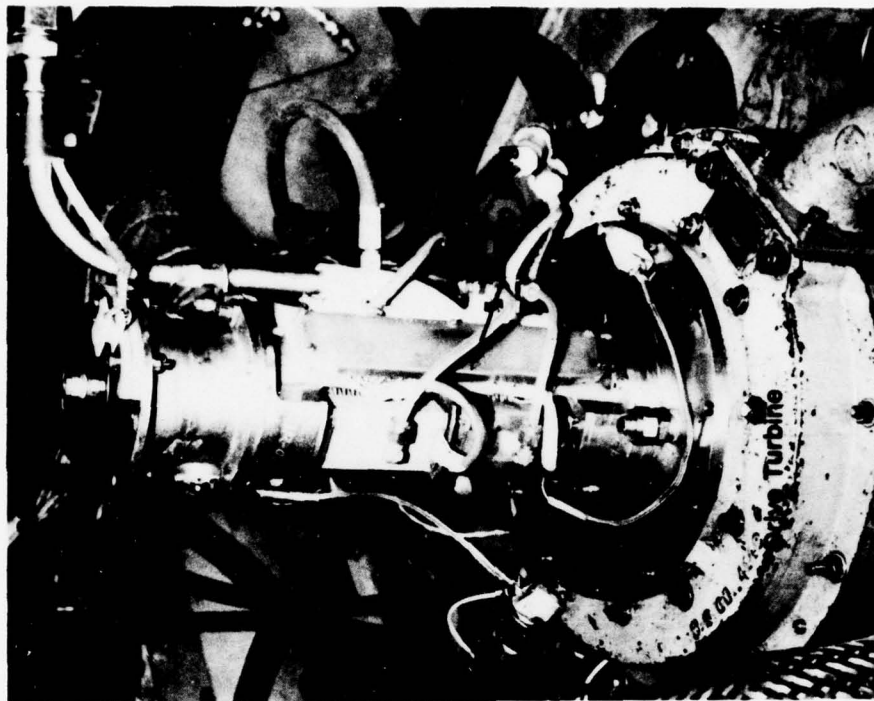
PROPOSED PWA SPIN PIT CONFIGURATION

FD 147960

Figure 9. Present and Proposed PWA Spin Pit Configurations



Setup for Image Derotated  
Holography in Spin Pit Facility

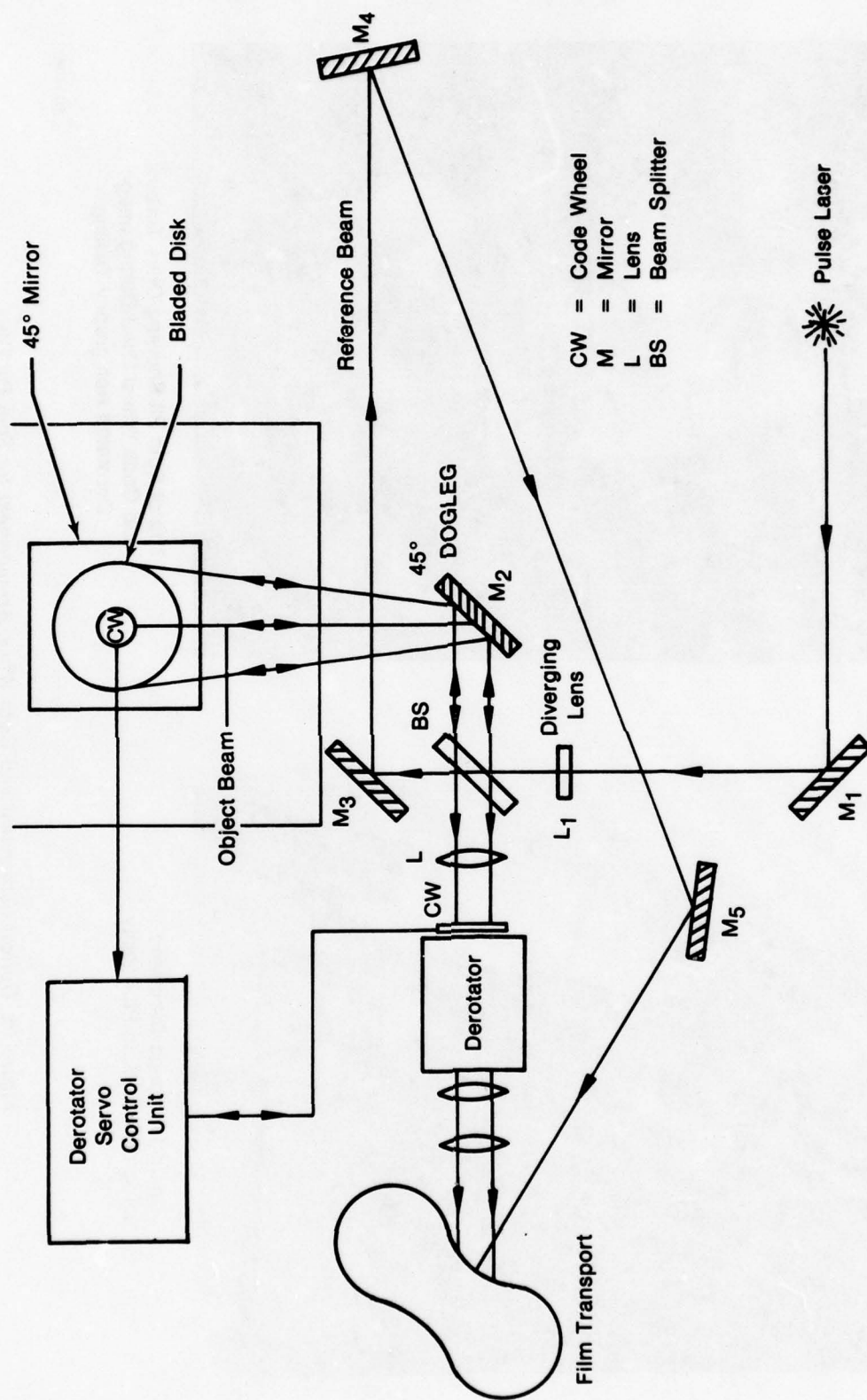


Top of Spin Pit Showing Drive Turbine  
and Code Wheel Used During Image  
Derotated Holography Testing

FD 147961

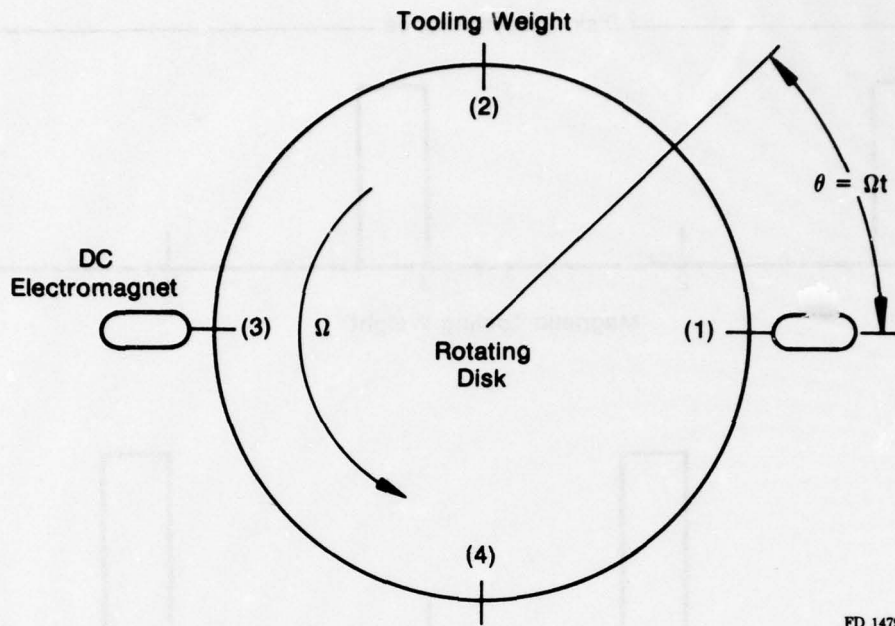
Figure 10. Optical Component and Code Wheel Arrangement for Spin Pit Tests





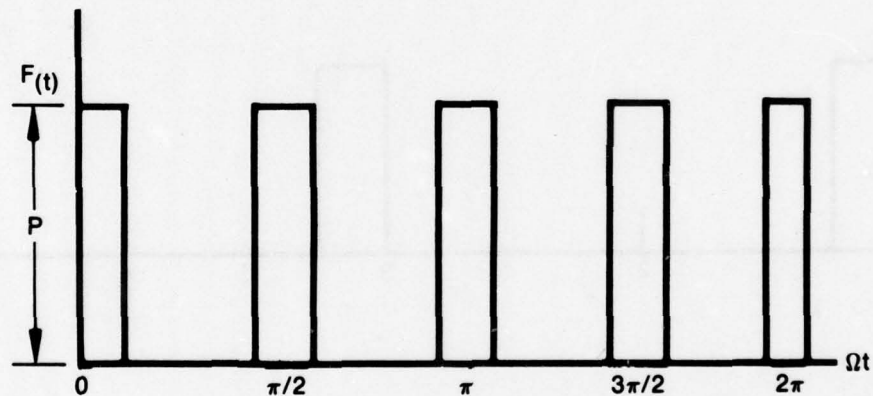
FD 147962

Figure 11. Experimental Setup for Image Derotated Holographic Interferometry in a Spin Pit Facility



FD 147963

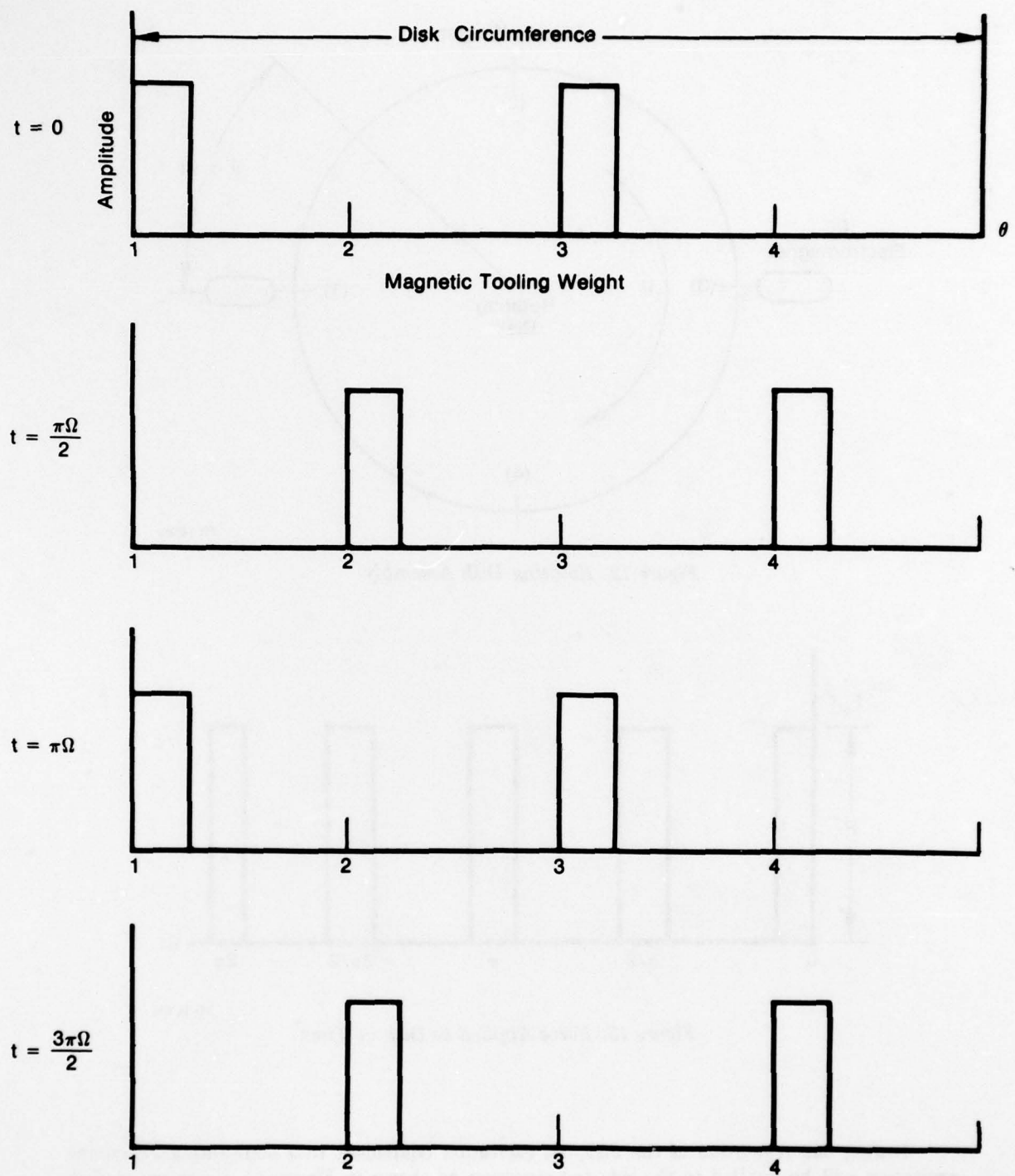
Figure 12. Rotating Disk Assembly



FD 147964

Figure 13. Force Applied to Disk vs Time

During one revolution of the disk, an excitation equivalent to a nonrotating 2E engine excitation will be applied to the rotating structure as shown in Figure 14. If the entire disk circumference were magnetic, the force on the disk would be constant. However, for the structure analyzed, this was not the case, therefore, a force was applied to the structure only when a diametrically opposed pair of magnetic tooling weights are opposite two of the magnets or four times per revolution as shown in Figure 14. It has been shown by J. MacBain through a Fourier series that the pulse train shown in Figure 13 has frequency components where  $\omega = 4\Omega, 8\Omega, 12\Omega, \dots, 4K\Omega$  where  $K =$  a positive integer.



FD 147965

Figure 14. Applied Disk Force vs Position of Force Application During One Disk Revolution



As shown previously, for a rotating disk acted upon by a nonrotating force of frequency,  $\omega$ , a disk resonant mode at a response frequency  $P_n$  is excited when:

$$P_n = \omega \pm \Omega n$$

where:

- $\omega$  = Forcing frequency (Hz)
- $\Omega$  = Disk angular velocity (RPS)
- $n$  = Mode nodal diameter

For the case under discussion where forcing frequencies,  $\omega = 4K\Omega$  exist, a resonant frequency  $P_n$  for the  $n^{\text{th}}$  diameter mode will be excited when  $P_n = \omega \pm n\Omega = 4K\Omega \pm n\Omega$  or:

$$P_n = [4K \pm n] \Omega \quad (4)$$

During each test period the assembly response frequencies were established through on-line analysis of the output signals from strain gages located on each of the four blades installed in the 2nd-stage disk as previously described. Rotational velocities which produced the greatest response amplitudes at each response frequency were established by the application of a tracking filter with a constant bandwidth of 10 Hz and a manually adjusted tuning frequency. At each response frequency, the unfiltered strain gage output signal from at least three strain gage locations was recorded and a Power Spectral Density (PSD) analysis conducted to establish frequency components of this complex signal. This analysis shows considerable slip ring noise at frequencies of  $E, 2E, \dots, nE$  where  $n$  = an integer, however, the response of the test structure is primarily at one predominant frequency. This was proven by the fact that the disk response frequency disappears when the magnetic excitation force is removed.

## DATA ANALYSIS

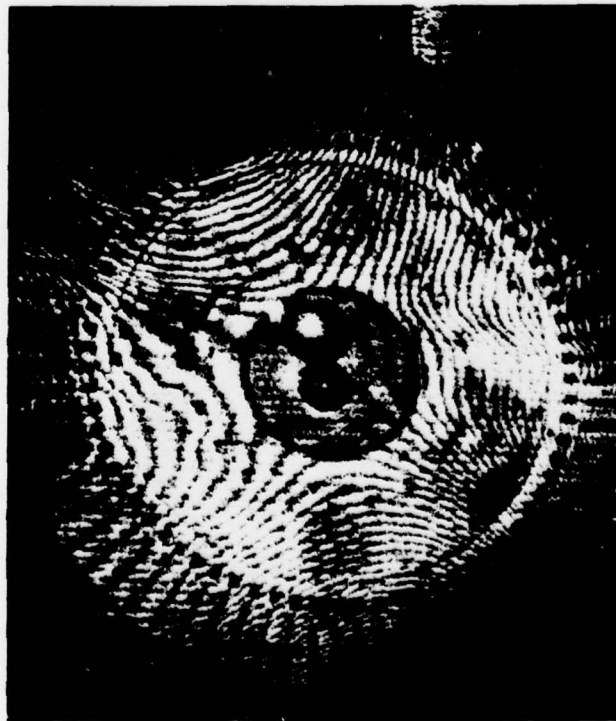
During each of the two test periods, double pulsed interferometric holograms of the rotating-vibrating test structure were constructed at a laser pulse separation of 30 to 40  $\mu\text{s}$  for each response frequency at various test structure angular velocities. These response frequencies and corresponding angular velocities are shown in Table 3. Photographs of typical reconstructed holograms are shown in Figures 15 through 17. The reconstructed holograms are relatively sharp in detail of the disk assembly, however, the large bias fringe density is still such that it is difficult to establish the mode shapes resulting at each response frequency established.

Even though the test structure was partially disassembled to repair strain gage leads, repeatability of the response frequencies established during each test period was excellent.

Rotational velocities of the test structure at which various preselected modes of vibration could be excited were calculated based on analysis of the response frequencies established for the nonrotating test structure in Section III and Equation (4) in this section. A plot of the various response frequencies established as a function of structure rotational velocity during the spin pit tests is shown in Figure 18. Lines of constant  $P_n/\Omega$  are drawn and values of  $m$  and  $k$  from Equation (4) which would satisfy this equation are shown. Also based on analysis of the test data, the probable test structure resonant frequency as a function of rpm for the various modes similar to a Campbell diagram are shown. Typical spectral plots of unfiltered signals, from strain gages mounted on the F100 second-stage turbine blades, as shown in Figure 3, are shown in Figures 19 through 23 for several rotational velocities with corresponding test structure response frequencies noted.

**TABLE 3**  
**DYNAMIC DATA DEVELOPED FOR AN F100 HIGH**  
**TURBINE TEST STRUCTURE IN A CONTROLLED**  
**SPIN PIT FACILITY**

<i>Test Structure Angular Velocity <math>\Omega</math> = rev/sec</i>	<i>Test Structure Response Frequency, <math>P_n</math> (Hz)</i>	<i><math>P_n/\Omega</math></i>	<i>Probable Mode Definition</i>	<i>Reference Figure No.</i>
98.3 (5900 rpm)	980	10	Blade alone 1st bending	16
127.5 (7650 rpm)	765	6	2 Nodal Dia	15
126.0 (7560 rpm)	756	6	2 Nodal Dia	15
74.5 (4470 rpm)	745	10	2 Nodal Dia	15
96.8 (5810 rpm)	967	10	Blade alone 1st bending	16
113.6 (6820 rpm)	1135	10	6 Nodal Dia	17
127.5 (7650 rpm)	765	6	2 Nodal Dia	15
128.3 (7700 rpm)	770	6	2 Nodal Dia	15
120.0 (7200 rpm)	960	8	4 Nodal Dia	16
99.0 (5940 rpm)	990	10	Blade alone 1st bending	16
113.6 (6810 rpm)	1135	10	6 Nodal Dia	17



FE 100040-10

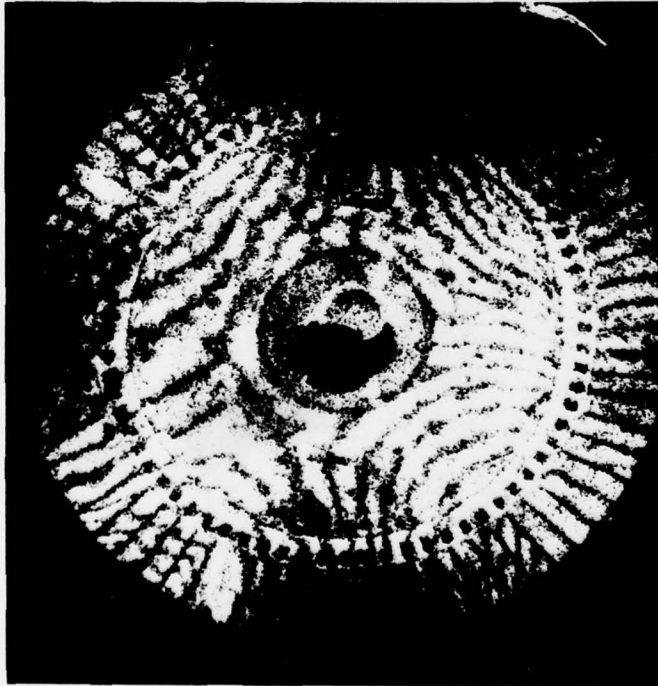


FREM 100770-10

FD 147966

Figure 15. Reconstructed Holograms of F100 High Turbine Rotor Assembly Taken With Assembly Rotating at 7650 rpm (Left) and 7700 rpm (Right) With Response Frequencies of 765 Hz and 770 Hz, Respectively





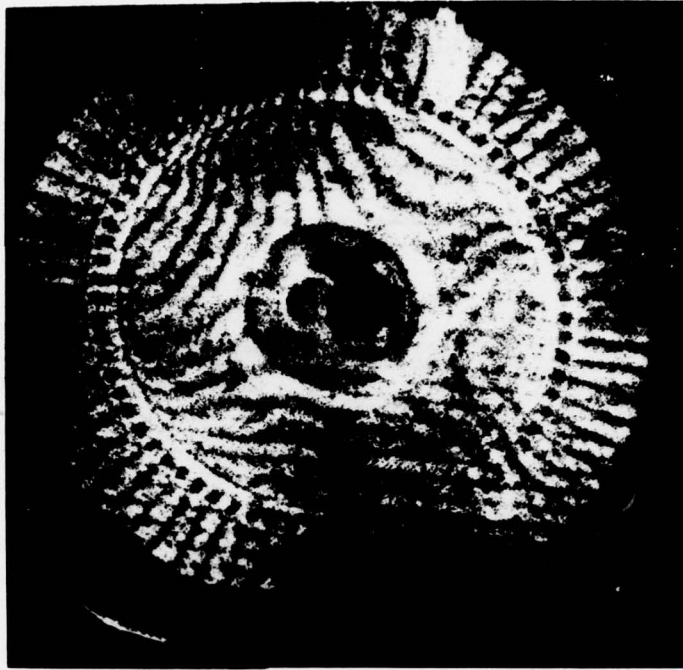
FXEH 100779-17



FE 100848-10

FD 147967

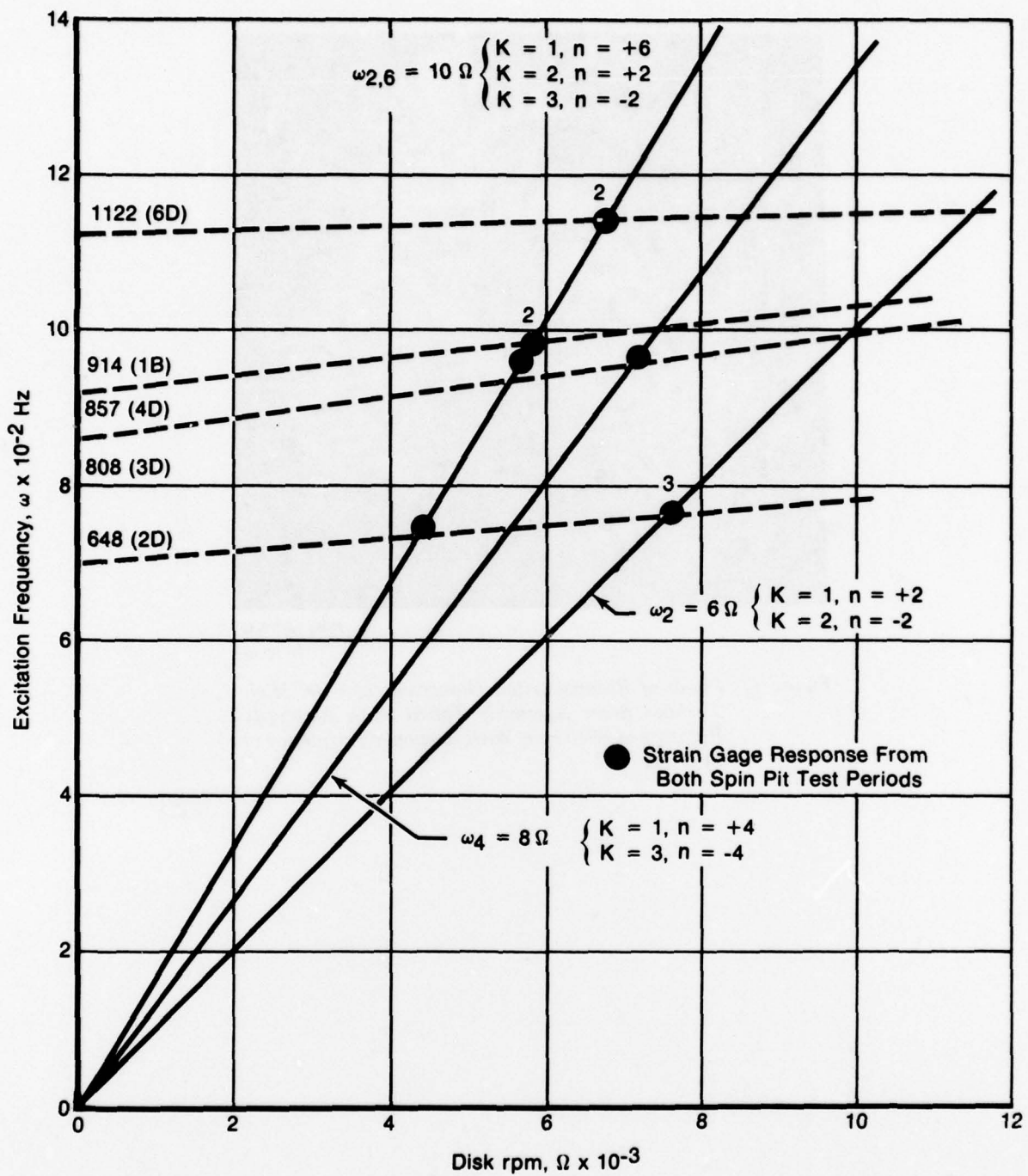
Figure 16. Reconstructed Holograms of F100 High Turbine Rotor Assembly Taken With Assembly Rotating at 7200 rpm (Left) and 5930 (Right) With Response Frequencies of 960 Hz and 990 Hz, Respectively



FXEH 169779-12

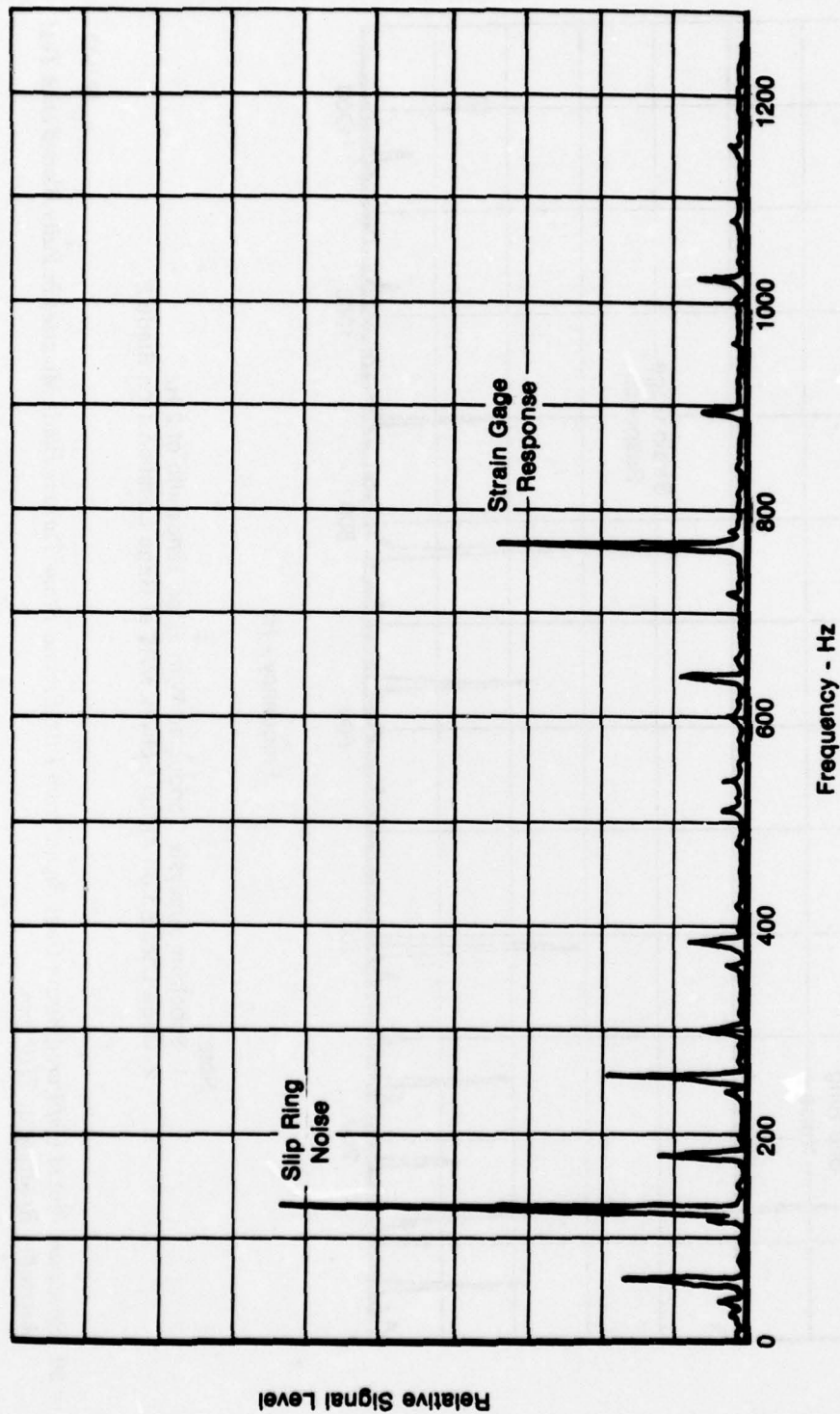
FD 147968

*Figure 17. Photo of Reconstructed Holograms of F100 High Turbine Rotor Assembly Taken With Assembly Rotating at 6810 rpm With Response Frequency of 1137 Hz*



FD 147969

Figure 18. Relation of Resonant Excitation Frequency as a Function of Test Structure Rotational Speed for Modes 2D, 4D, 6D and Blade Alone First Bending and Resonant Response Frequency as a Function of Increasing Speed



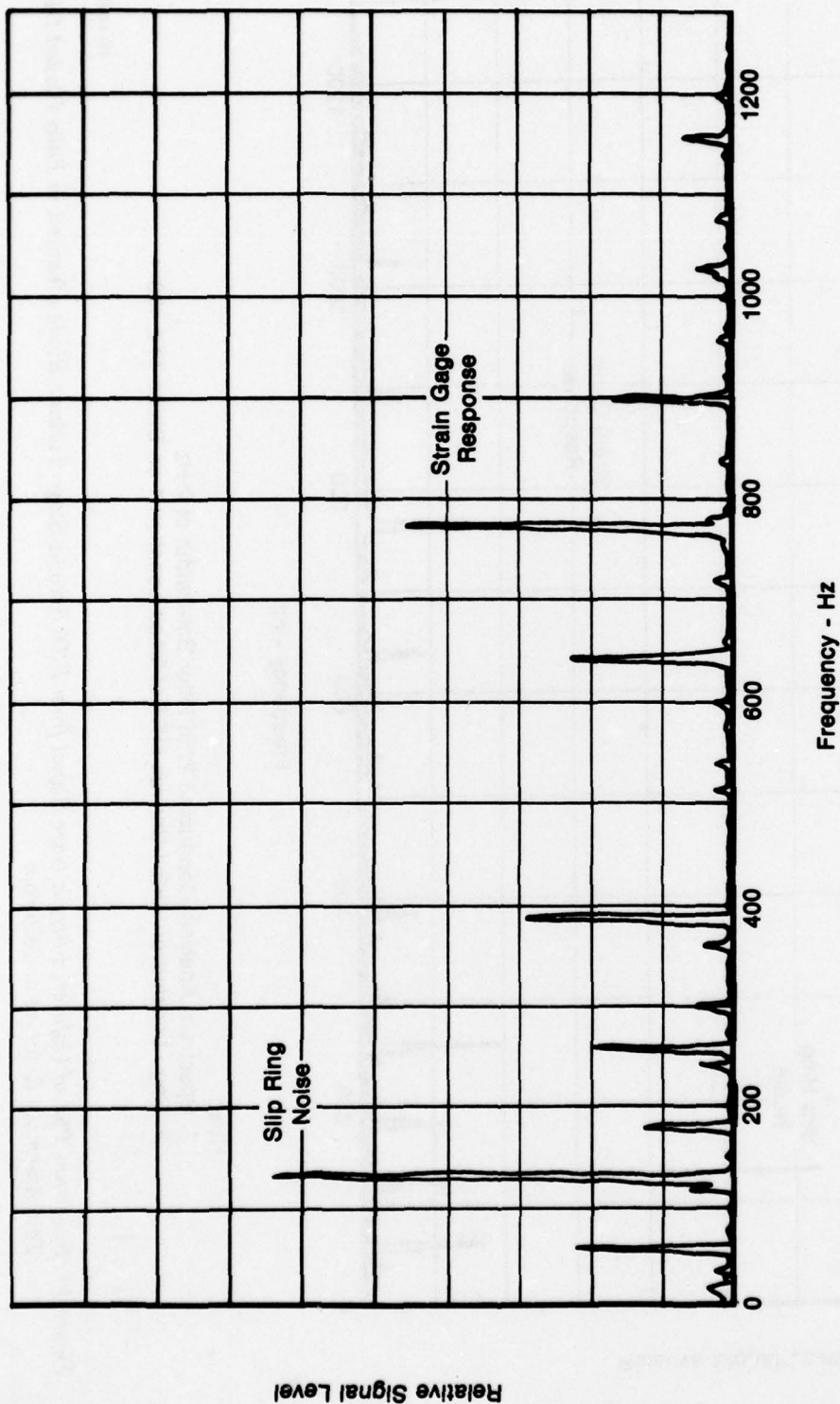
**Note:**

1. Spectrum Analysis Conducted With Filter Bandwidth of 2 Hz
2. Gage Located on Airfoil Convex MRT at Gage Location 1 on Blade TTE 430

FD 147970

**Figure 19. Spectrum Plot of Unfiltered Strain Gage Signal from F100 Second-Stage Turbine Blade Mounted in Fully Bladed Disk Test Assembly Rotating at 7650 rpm**



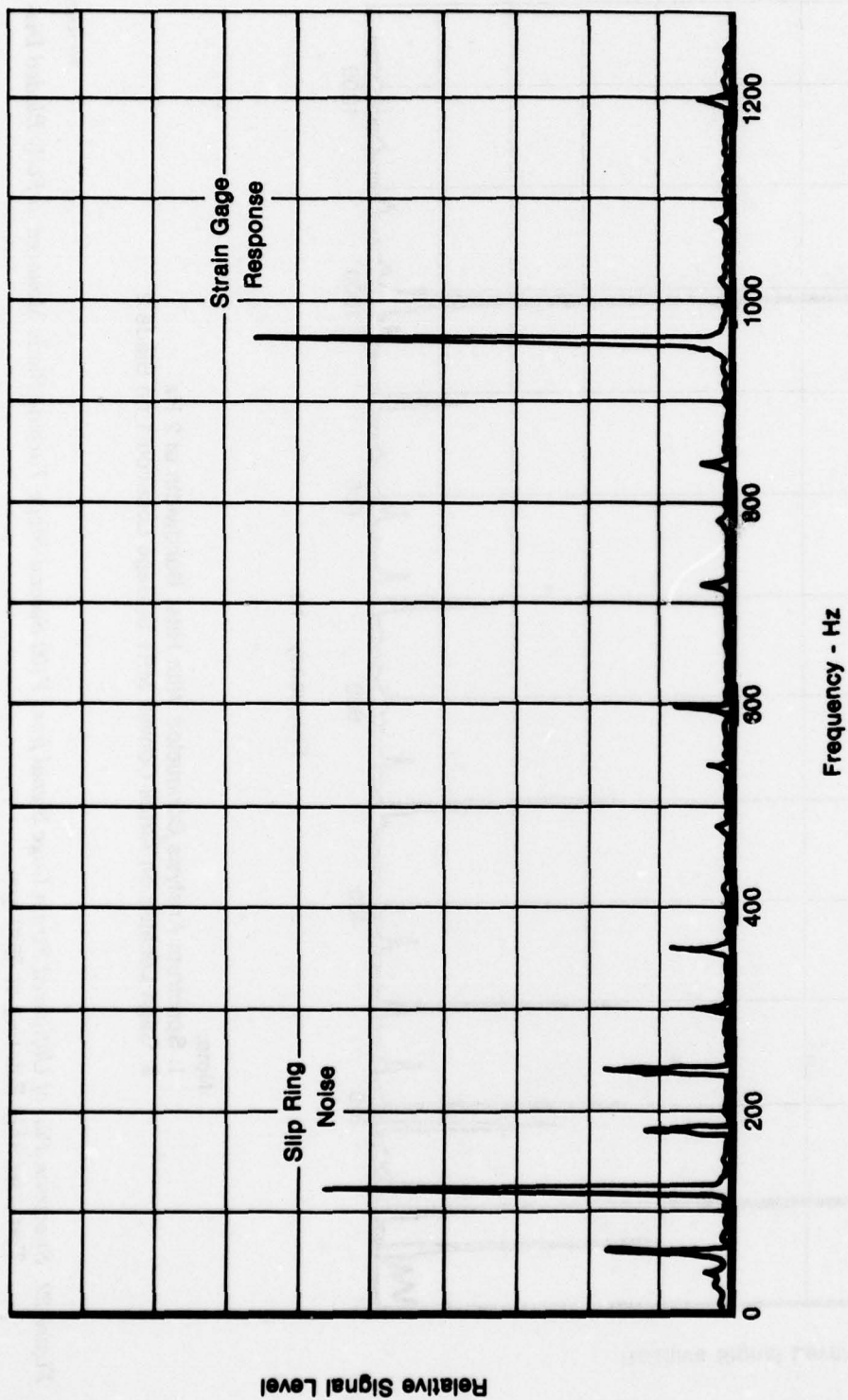


**Note:**

1. Spectrum Analysis Conducted With Filter Bandwidth of 2 Hz
2. Gage Located on Airfoil Convex MRT at Gage Location 1 on Blade 2

FD 147971

**Figure 20. Spectrum Plot of Unfiltered Strain Gage Signal from F100 Second-Stage Turbine Blade Mounted in Fully Bladed Disk Test Assembly Rotating at 7710 rpm**

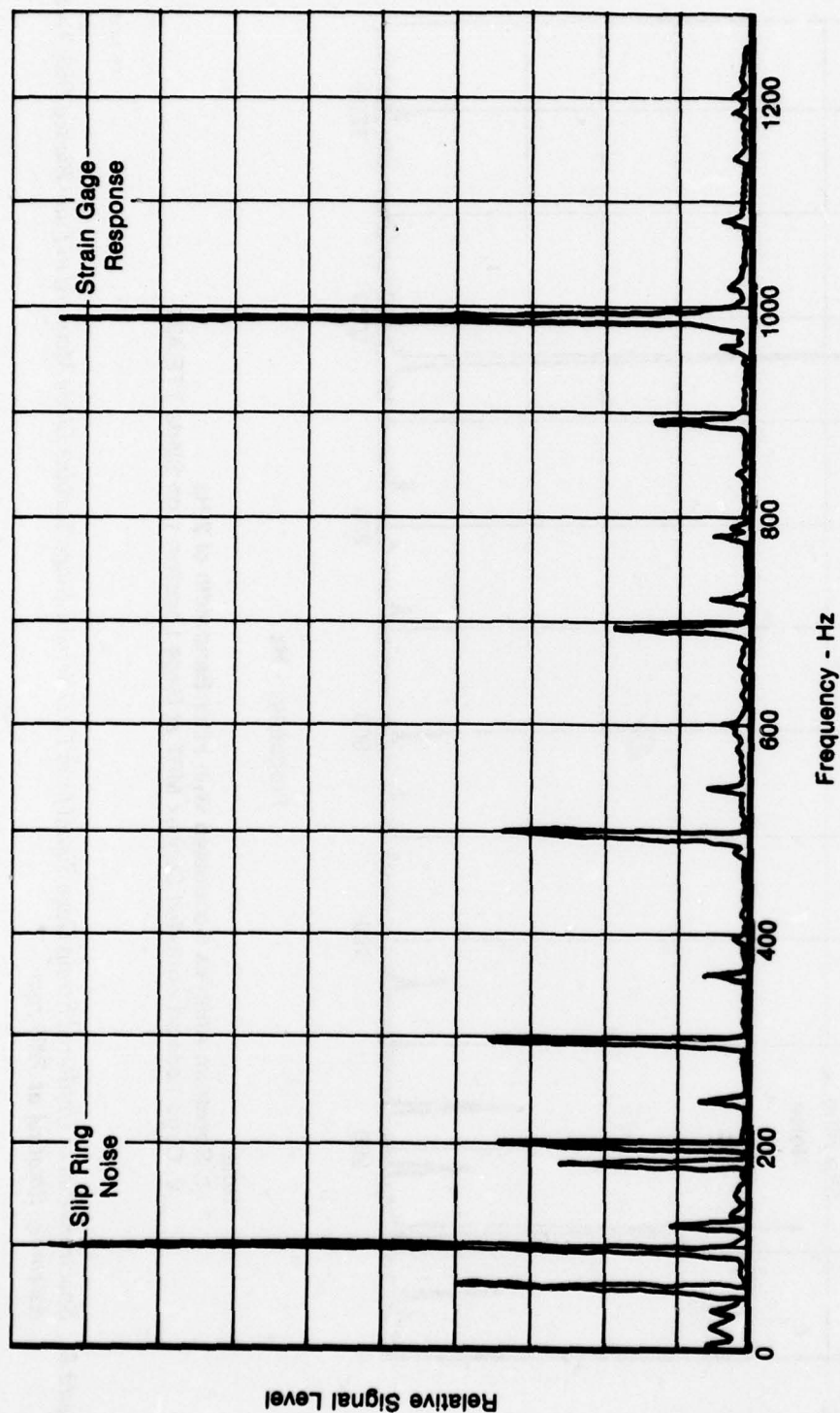


Note:

1. Spectrum Analysis Conducted With Filter Bandwidth of 2 Hz
2. Gage Located on Airfoil Convex MRT at Gage Location 1 on Blade TTE 430

FD 147972

Figure 21. Spectrum Plot of Unfiltered Strain Gage Signal from F100 Second-Stage Turbine Blade Mounted in Fully Bladed Disk Test Assembly Rotating at 7200 rpm



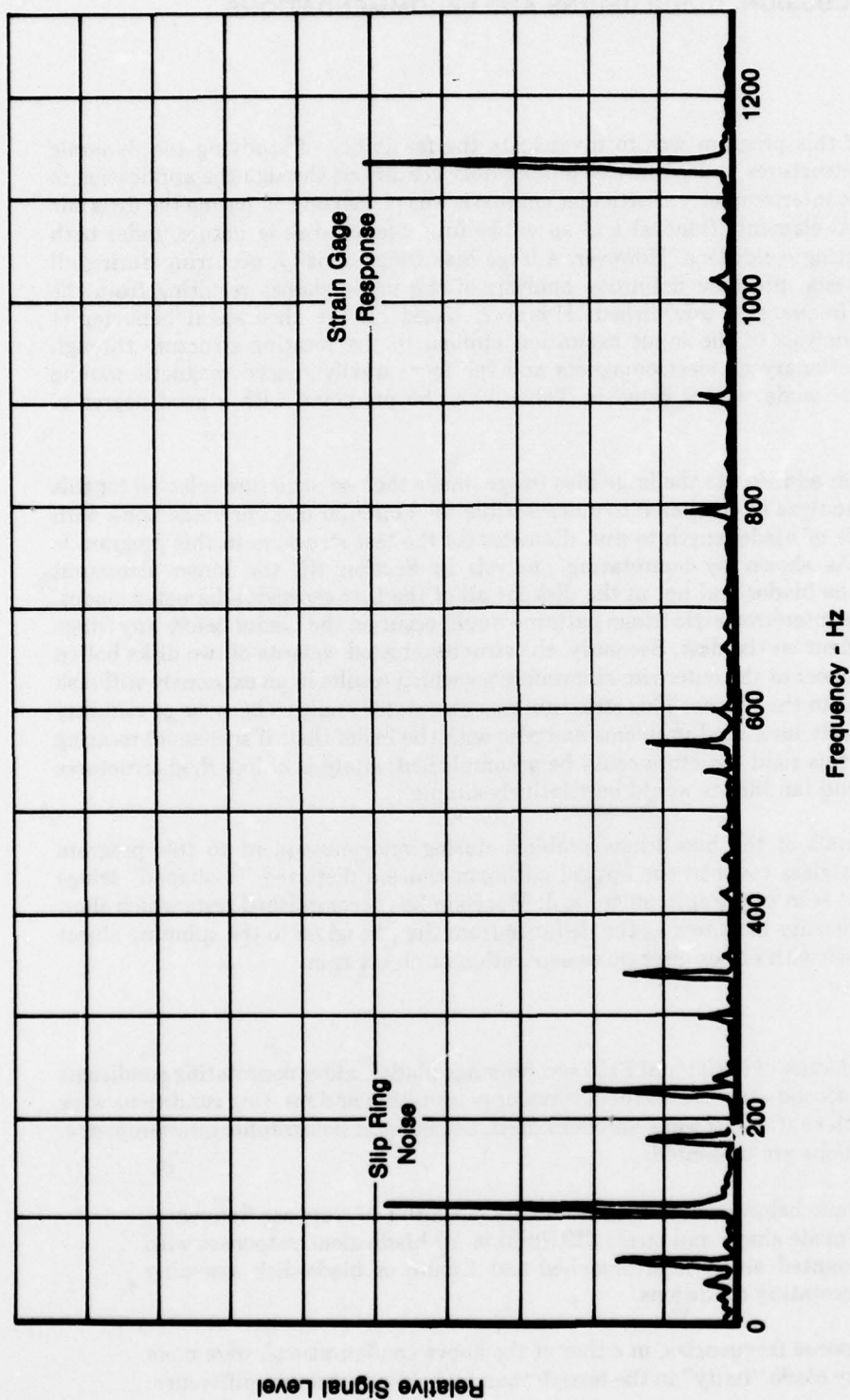
**Note:**

1. Spectrum Analysis Conducted With Filter Bandwidth of 2 Hz
2. Gage Located on Airfoil Convex MRT at Gage Location 1 on Blade 2

FD 147973

**Figure 22. Spectrum Plot of Unfiltered Strain Gage Signal from F100 Second-Stage Turbine Blade Mounted in Fully Bladed Disk Test Assembly Rotating at 5930 rpm**





**Note:**

1. Spectrum Analysis Conducted With Filter Bandwidth of 2 Hz
2. Gage Located on Airfoil Convex MRT at Gage Location 1 on Blade TSS 43

FD 147974

**Figure 23. Spectrum Plot of Unfiltered Strain Gage Signal from F100 Second-Stage Turbine Blade Mounted in Fully Bladed Disk Test Assembly Rotating at 6810 rpm**



## SECTION V

### DISCUSSION, CONCLUSIONS AND RECOMMENDATIONS

#### DISCUSSION

The purpose of this program was to investigate the feasibility of studying the dynamic behavior of rotating structures under controlled laboratory conditions through the application of derotated holographic interferometry. Particular emphasis was placed on comparing the dynamic behavior of individual elements (blades) and an entire fully bladed disk structure under both nonrotating and rotating conditions. However, a large bias fringe density, occurring during all periods of rotating tests, preclude definitive analysis of the mode shapes resulting from the structural response frequencies established. However, based on the theoretical behavior of circular disks and analysis of the input excitation applied to the rotating structure through interaction of the stationary dc electromagnets and the four equally spaced magnetic tooling weights, the resultant mode shapes listed in Table 3 can be predicted with a good degree of confidence.

Several factors in addition to the large bias fringe, make the test structure selected for this program difficult to analyze as compared to more flexible solid circular disks or bladed disk with long blades. The ratio of blade length to disk diameter for the test structure in this program is approximately 1:7. As shown by nonrotating analysis in Section III, the larger structural deflections occur in the blades and not in the disk for all of the first six nodal diameter modes. This means that large interferometric fringe patterns would occur on the blades before any fringe pattern would be evident on the disk. Secondly, the structure tested consists of two disks bolted together with a rim spacer at the outer rim circumference which results in an extremely stiff disk structure as compared to the blades. This structure was chosen for analysis because of visibility resulting from previously identified problems and also with the belief that, if successful rotating dynamic behavior of this rigid structure could be accomplished, analysis of less rigid structures such as compressor and fan blades would be relatively simple.

Additional analysis of the bias fringe problem during and subsequent to this program indicate that the plexiglass cover in the optical path can cause a distorted "Y-shaped" fringe pattern typical of that seen in the spin pit tests. J. MacBain has accomplished tests which show that this bias fringe density increases as the distance from the plexiglass to the spinning object decreases and increases with either laser pulse separation or object rpm.

#### CONCLUSIONS

The dynamic behavior of individual F100 second-stage blades under nonrotating conditions and of a fully bladed second-stage test structure under nonrotating and rotating conditions were investigated using both continuous wave and derotated, pulsed laser holographic interferometry. The following conclusions are presented:

1. The dynamic behavior of individual blades is similar in response frequency, resultant mode shape and stress distribution for blade alone responses with blades mounted either in a broached test fixture or blade-disk assembly under nonrotating conditions.
2. Blade response frequencies, in either of the above configurations, were more affected by blade "fixity" in the broach than by holding structure difference.

3. As expected, centrifugal loading of the bladed-disk test structure resulted in increasing response frequencies as shown in Figure 18. Figure 18 also shows the feasibility of developing experimental Goodman diagrams (structural response frequency vs rotational velocity) for various modes in a spin pit facility.
4. Electromagnetic excitation of bladed-disk structures is practical and by application of the relation  $P_n = (K \pm n) \Omega$  all principal modes can be excited by the proper spatial arrangement of magnets and tooling weights.
5. Optical derotated, pulsed laser holographic interferometry in a controlled spin pit facility for the study of bladed-disk dynamic behavior is feasible as shown by the holograms constructed during this program.
6. The degree of feasibility is directly related to the ability to produce sufficient vibratory amplitude in the test structure and to eliminate the undesirable bias fringe density.

### RECOMMENDATIONS

Significant progress in applying derotated interferometric holography in a controlled spin pit facility has been achieved during this program. Although some technical problems have been identified and the constructed rotating holograms are not sufficiently definitive regarding resultant mode shapes, the results are encouraging. Pratt & Whitney Aircraft Group, Government Products Division is currently building a new spin pit facility which will be modified as shown in Figure 9 to remove the plexiglass vacuum can cover from the optical path. As previously noted, this should relieve the large bias fringe problem. To relieve the problem of a very rigid test structure it is recommended that a less flexible test structure such as an F100 4th-stage compressor bladed-disk be used in any subsequent investigations along with improved excitation.

In view of the significant progress accomplished during this program, it is recommended that this investigation be continued either under this or an additional program based on the above recommendations.

## REFERENCES

1. Stetson, K. A. and J. N. Elkins, *Optical System for Dynamic Analysis of Rotating Structures*, AFAPL-TR-77-51 AD A050-758, Contract F33615-C-2013, Oct. 1977.
2. Bearden, J. L. and J. J. Weber, "Feasibility Study of Various Methods to Induce Vibratory Excitation of Engine Blades Centrifugally Loaded," FMDL 19491, 1976.
3. Stetson, K. A., "The Use of Image Derotation in Holographic Interferometry and Speckly Photography of Rotating Objects," *Experimental Mechanics*, Vol. 18(2), pp. 67-73, 1978.
4. Timoshenko, S., *Vibration Problem in Engineering*, Third Edition, pp. 455-461, 1955.
5. MacBain, J., J. Horner, W. Stange, and J. Ogg, "Vibration Analysis of a Spinning Disk Using Image Derotated Holographic Interferometry," Paper presented at SESA Spring Meeting, Wichita, Kansas, 1978.
6. Campbell, W. E., "The Protection of Steam Turbine Disc Wheels from Axial Vibration," ASME Spring Meeting, Cleveland, May 1924.